

Review of Conjunction Probability Methods for Short-term Encounters

Salvatore Alfano*

Center for Space Standards and Innovation, Colorado Springs, Colorado, 80132

This paper discusses current methods for computing collision probability between spaceborne objects. Current formulations are based on the Gaussian distribution and the concept of covariances which can be obtained from orbit determination. In broad general terms and in chronological order, there are four main categories to classify the current models. These are the Foster (1992), Chan (1997), Patera (2001 & 2005) and Alfano (2005) models. This work compares the numerical results obtained from those four algorithms with validation results obtained using the MATHCAD solution of the two-dimensional probability integral over a very wide range of collision parameters (miss distance, standard deviations and collision cross-section radius). Based on the number of function evaluations which is an indication of computing efficiency, the Foster model is approximately ten or twenty times slower than either the Alfano or Patera model, which in turn are orders of magnitude slower than the Chan model. Within the prescribed bounds of testing, the models typically are accurate to two or more significant figures.

Nomenclature

erf	= error function
k	= power series term
m	= power series term
n	= covariance ellipsoid scale factor or power series term
OBJ	= combined object radius
R	= miss distance
r	= integration variable (object radius)
U	= principal axis in encounter plane
W	= principal axis in encounter plane
x	= distance along minor axis
xm	= miss distance along minor axis
y	= distance along major axis
ym	= miss distance along major axis
ϕ	= miss distance angle relative to ellipse primary axis
σ	= standard deviation
θ	= integration variable (angle)

* Technical Program Manager, CSSI, 7150 Campus Drive, Suite 260, Colorado Springs, CO, 80920-6522, salfano@centerforspace.com, AIAA Associate Fellow.

I. Introduction

This paper discusses four current methods to compute collision probability for short-term encounters between space-borne objects. The early formulations of spacecraft collision were based on the Poisson distribution and used concepts from the kinetic theory of gases in which the molecules move in straight lines and their number density is statistically uniform. Current formulations are more realistic, being based on the positional Gaussian distribution and the concept of covariances which can be obtained from orbit determination. In broad general terms and in chronological order, the four main models were developed by Foster¹, Chan², Patera³, and Alfano⁴.

The method developed by Foster¹ for NASA evaluates the collision probability numerically by examining the plane perpendicular to relative motion, dividing the combined object's circular cross-section in concentric circles and radial straight lines. The model developed by Chan² is analytical, being based on transforming the two-dimensional Gaussian probability density function (pdf) to a one-dimensional Rician pdf and using the concept of equivalent areas. This model involves the evaluation of an analytical expression containing two exponential terms. The Patera³ model is based on a one-dimensional pdf and is formulated in the form of a "line-integral." Its evaluation is performed numerically by taking short line segments around a closed contour. The Alfano⁴ model is also based on a one-dimensional pdf expressed as two error functions and one exponential term. It is numerically evaluated using well-known software already developed for error functions.

This paper presents a comparison of numerical results obtained from those four models against a suite of test cases. The reference (truth) probability was computed with MATHCAD 13 set to the highest tolerance that would still allow convergence of the double integral. This investigation serves to check the validity and accuracy of the models as pure modules against the reference probability without introducing extraneous activities such as the propagation of the state vectors, the determination of the closest distance at conjunction, and the propagation of the combined covariance as prerequisites. For a very wide range of collision parameters (miss distance, standard deviations, and collision cross-section radius) covering collision probabilities in the range of 0.1 to 10^{-7} , the four models are almost always in good agreement. Using the number of function evaluations as an indicator of computational efficiency, the fastest model is Chan's and the slowest is Foster's. The Alfano and Patera models are relatively close in computing speeds.

II. Probability computation

A. General Method

The assumptions involved in linear collision probability formulation are well defined in References 1-4 and are summarized here for the reader's convenience. Space object collision probability analysis (COLA) is typically conducted with the objects modeled as spheres, thus eliminating the need for attitude information. Their relative motion is considered linear for the encounter by assuming the effect of relative acceleration is dwarfed by that of the velocity. The positional errors are assumed to be zero-mean, Gaussian, uncorrelated, and constant for the encounter. The relative velocity at the point of closest approach is deemed sufficiently large to ensure a brief encounter time and static covariance. The encounter region is defined when one object is within n standard deviations ($n\sigma$) of the combined covariance ellipsoid. This user-defined, three-dimensional, $n\text{-}\sigma$ shell is centered on the primary object; n is typically in the range of 3 to 8 to accommodate conjunction possibilities ranging from 97.070911% to 99.999999%.

Because the covariance matrices are expected to be uncorrelated, they are simply summed to form one, large, combined, covariance ellipsoid that is centered at the primary object. The secondary object passes quickly through this ellipsoid creating a tube-shaped path that is commonly called a collision tube. A physical overlap occurs if the secondary sphere comes within a distance equal to the sum of the two radii. Thus, we have a condition for collision. The probability of collision is obtained by evaluating the integral of the three-dimensional pdf within a long circular cylinder. It can be shown that this is equivalent to evaluating the integral of the two-dimensional pdf within a circle on a plane perpendicular to the relative velocity at closest approach. This is illustrated in the following figure.

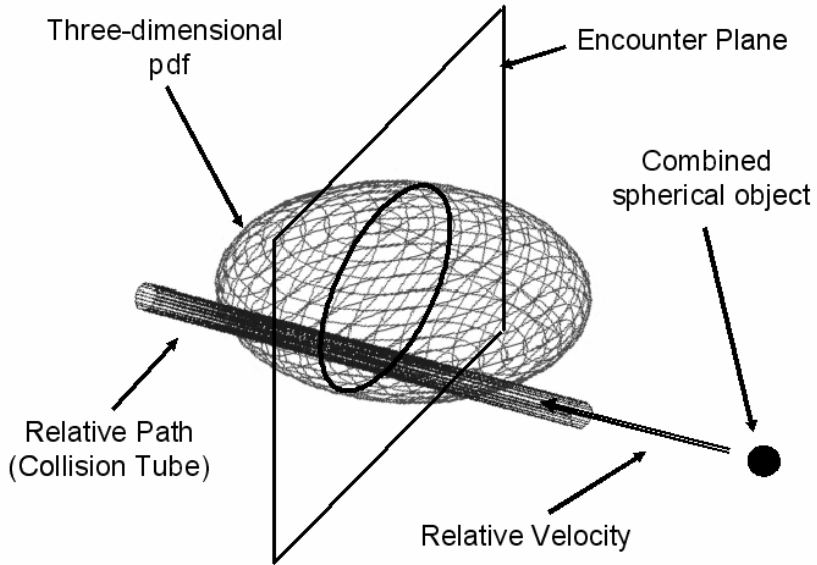


Fig. 1 Conjunction Encounter Visualization

As previously stated, the encounter region is defined by an $n\text{-}\sigma$ shell determined by the user to sufficiently account for conjunction possibilities. For short-term encounters⁵, the tube is assumed straight and rapidly traversed, allowing a decoupling of the dimension associated with the tube path (relative velocity). The tube becomes a circle on the projected encounter plane. Likewise, the covariance ellipsoid becomes an ellipse as depicted in Figure 2.

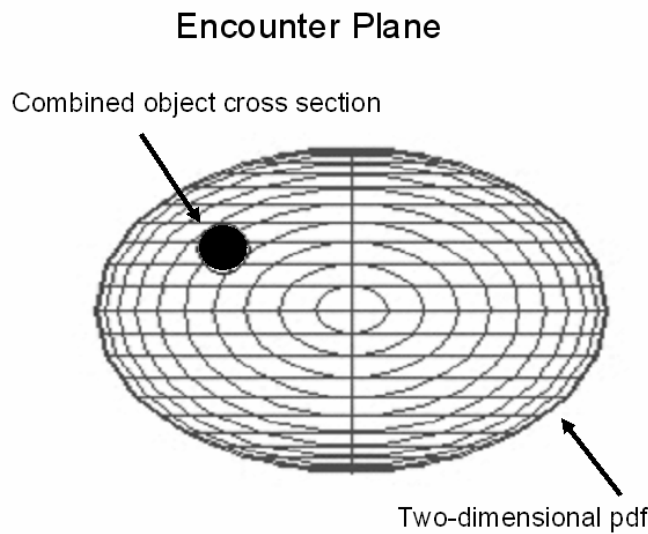


Fig. 2 Combined Covariance Sliced by Encounter Plane

The relative velocity vector (decoupled dimension) is associated with the time of closest approach. The conjunction assessment here is concerned with cumulative probability over the time it takes to span the $n\text{-}\sigma$ shell, not an instantaneous probability at a specific time within the shell. Along this decoupled dimension, integration of the probability density across the shell produces a number very near unity, meaning the close approach will occur at some time within the shell with near absolute certainty. Thus the cumulative collision probability is reduced to a two-dimensional problem in the encounter plane that is then multiplied by the decoupled dimension's probability. By rounding the latter probability to one, it is eliminated from further calculations. Thus the projection results in a double integral.

The resulting two-dimensional probability equation in the encounter plane is given in Cartesian space as

$$P = \frac{1}{2 \cdot \pi \cdot \sigma_x \cdot \sigma_y} \cdot \int_{-OBJ}^{OBJ} \int_{-\sqrt{OBJ^2-x^2}}^{\sqrt{OBJ^2-x^2}} \exp \left[\frac{-1}{2} \cdot \left[\left(\frac{x-xm}{\sigma_x} \right)^2 + \left(\frac{y-ym}{\sigma_y} \right)^2 \right] \right] dy dx \quad (1)$$

where OBJ is the combined object radius, x lies along the minor axis, y lies along the major axis, xm and ym are the respective components of the projected miss distance, and σ_x and σ_y are the corresponding standard deviations. The four methods examined in this paper express Equation 1 numerically (Foster, Patera, Alfano) or by analytical approximation (Chan).

This investigation is an extension of Chan’s previously published comparisons.⁶ It serves to check the validity and accuracy of the methods against a truth model without introducing extraneous activities such as the propagation of the state vectors, the determination of the closest distance at conjunction and the propagation of the combined covariance as prerequisites. All computations start in the encounter plane.

B. MATHCAD Implementation

Equation 1 was directly inserted into MATHCAD without alteration. The reference (truth) probability was then computed with MATHCAD 13 set to the highest tolerance that would still allow convergence of the double integral. For these validation cases the tolerance was set to 10^{-9} thereby guaranteeing accuracy to at least 9 decimal places. For this paper, an operational decision making region is outlined by a solid red line defining one percent error for collision probability ranging from 10^{-1} and 10^{-7} . Some users might consider this region too restrictive and perhaps accept up to a 10% difference or make the upper probability bound 10^{-3} . Ideally, the method should never produce results in this region, thus ensuring sufficient accuracy for decision-making. If an approximation does produce answers in this region, then it should overestimate (erring on the conservative side). An overestimate is represented with a blue plus sign and an underestimate is marked with a red x as shown in Figure 3.

Approximately 60,000 test cases were used to evaluate the probability equation. These cases had all parameters normalized to the covariance ellipse’s minor-axis standard-deviation of 1. The object size varied from 10^{-3} to 10^{+3} , the miss distance varied from 10^{-4} to 10^{+3} with position ranging from 0^0 to 90^0 relative to the minor axis, and the covariance ellipse’s major-axis standard-deviation varied from 1 to 500 ($1 \leq AR \leq 500$). These parameters go well beyond what is found in present day values. Because the truth results are good to at least 9 decimal places, differences beyond this accuracy might be attributed to MATHCAD and not the method being tested. A blue-dashed line outlines this validation data limit; differences above this line are due to inaccuracies in the tested method and not to MATHCAD. A set of figures with AR of 1, 2, 3, 5, 10, 50, and 500 can be found for all four methods in the Appendix A.

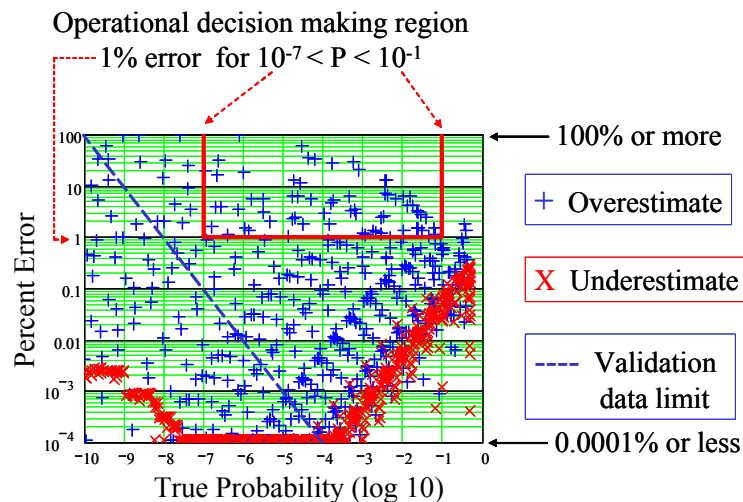


Figure 3. Chart legend for comparing a model to MATHCAD-generated validation results.

III. Foster's Method

A. General Method

Foster¹ derived a collision probability model using polar coordinates in the encounter (U-W) plane where R_0 and ϕ define the combined object center's location, OBJ is the combined object radius, σ_u and σ_w are the principal axes standard deviations, and r and θ define the relative spatial position of the segmented object.

$$P = \frac{1}{2 \cdot \pi \cdot \sigma_u \cdot \sigma_w} \int_0^{OBJ} \left[\int_0^{2 \cdot \pi} \exp \left[\frac{-1}{2} \cdot \left[\left(\frac{R_0 \cdot \sin(\phi) - r \cdot \sin(\theta)}{\sigma_u} \right)^2 + \left(\frac{R_0 \cdot \cos(\phi) - r \cdot \cos(\theta)}{\sigma_w} \right)^2 \right] \right] \cdot r \, d\theta \right] dr \quad (2)$$

In Foster's numerical implementation the angle ϕ is measured from the W axis, the angle θ step size is 0.5° , and the radius r step size is $OBJ/12$. This model is currently used by NASA to assess on-orbit risk for ISS and Shuttle missions. It can also be found in The Aerospace Corporation's Collision Vision Tool.

B. Numerical testing

Equation 2 was programmed in FORTRAN using the step sizes recommended in the NASA/JSC paper. During testing, certain cases placed the results inside the operational decision making region. Further investigation showed that these incursions occurred when the object radius was smaller than the miss distance but larger than the standard deviation of the minor axis. Within the accuracy bounds of currently available orbital data, it is reasonable to assume that these theoretical cases are highly unlikely. If needed, Foster's method can handle these cases by decreasing the step sizes of θ and r .

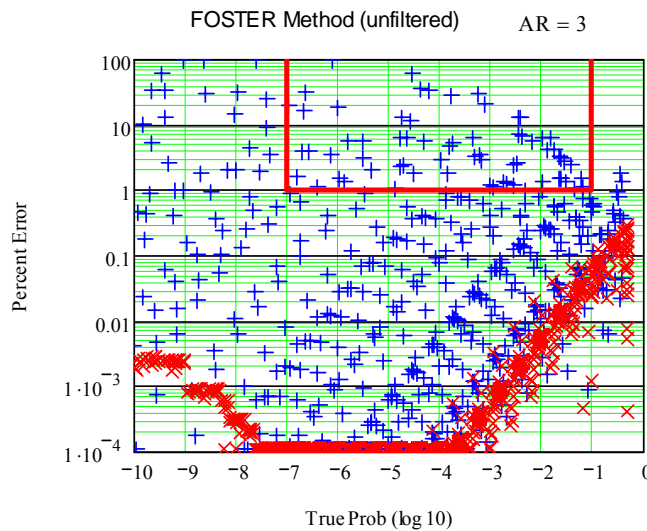


Figure 4a. Foster method (unfiltered) comparison with object smaller than or equal to miss distance

A complete set of unfiltered case results can be found in Appendix A.

The following figure shows the results of eliminating those cases where the object radius was smaller than the miss distance but larger than the standard deviation of the minor axis.

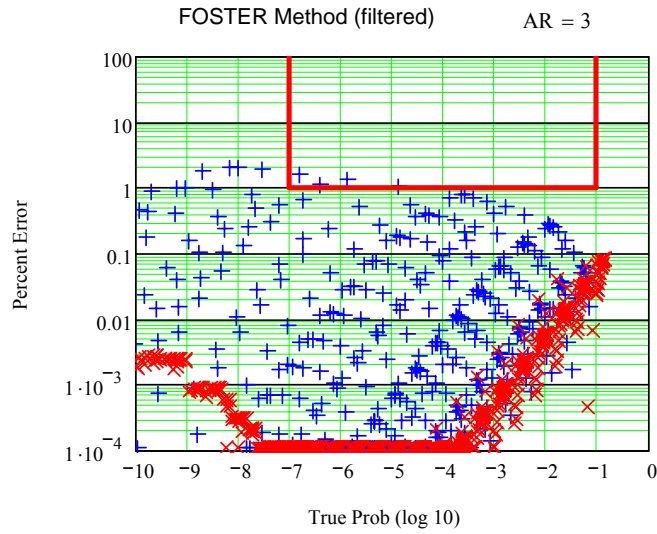


Figure 4b. Foster method (filtered) comparison with object smaller than or equal to miss distance

A complete set of filtered case results can be found in Appendix B.

IV. Chan's Method

A. General Method

Chan² developed a series expression as an analytical approximation to Equation 1 based on representative, present-day values ($1m \leq OBJ \leq 100m$, $10m \leq \text{miss distance} \leq 100KM$, $1KM \leq \sigma \leq 10KM$). Chan transforms the two-dimensional Gaussian probability density function (pdf) to a one-dimensional Rician pdf and uses the concept of equivalent areas. In the encounter plane, the combined object radius is OBJ, centered at (x_m, y_m) with associated standard deviations of (σ_x, σ_y) . The series expression is

$$P = \exp\left(\frac{-v}{2}\right) \cdot \sum_{m=0}^{\infty} \left[\frac{v^m}{2^m \cdot m!} \cdot \left(1 - \exp\left(\frac{-u}{2}\right) \cdot \sum_{k=0}^m \frac{u^k}{2^k \cdot k!} \right) \right] \tag{3a}$$

where

$$u = \frac{OBJ^2}{\sigma_x \cdot \sigma_y} \qquad v = \frac{x_m^2}{\sigma_x^2} + \frac{y_m^2}{\sigma_y^2} \tag{3b \& 3c}$$

This expression has the added benefit of being easily differentiated for other types of probability analysis. For this evaluation 11 terms were used ($m=10$). This model is currently implemented in Analytical Graphics, Inc., Satellite Tool Kit with 2 terms ($m=1$).

B. Numerical testing

Equations 3a, 3b, and 3c were programmed in FORTRAN. During testing, certain cases placed the results inside the operational decision making region. Further investigation showed that these incursions occurred when the object radius was larger than one-tenth of the smaller standard deviation. Increasing the number of terms will not correct these incursions because they result from the equivalent-area approximation.

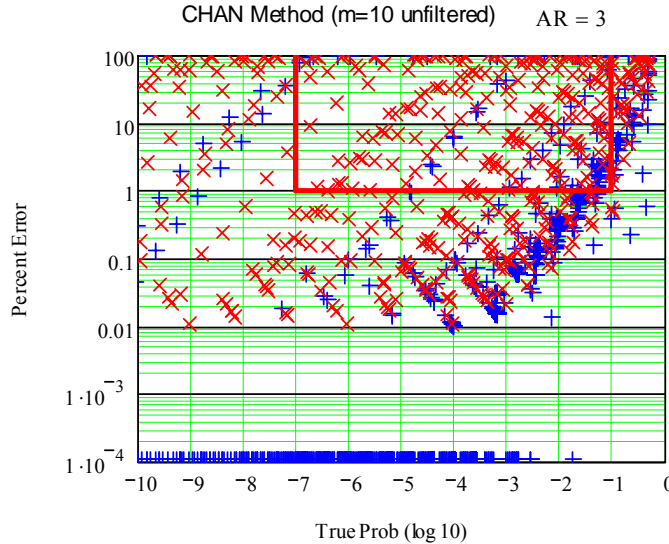


Figure 5a. Chan method (m=10, unfiltered) comparison with object smaller than or equal to miss distance

A complete set of unfiltered case results can be found in Appendix A.

The following figure shows the results of eliminating those cases where the object radius is larger than one-tenth of the smaller standard deviation. This is reasonable given the present accuracy of orbital data.

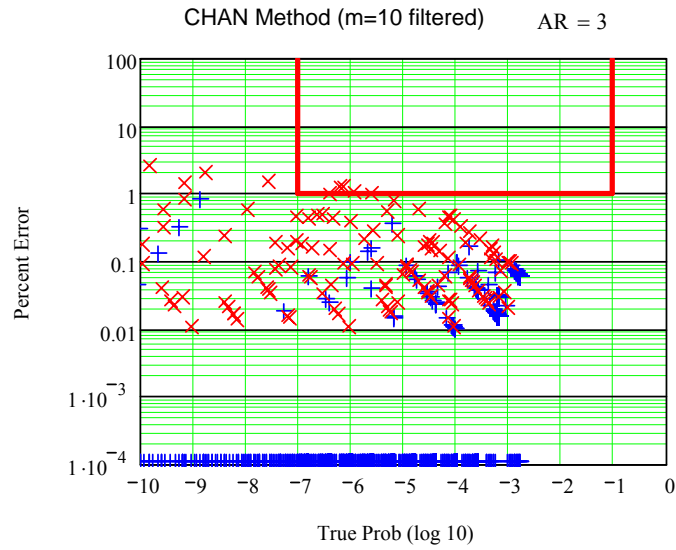


Figure 5b. Chan method (m=10, filtered) comparison with object smaller than or equal to miss distance

A complete set of filtered case results can be found in Appendix B.

V. Patera's Method

A. General Method

Patera³ developed a mathematically equivalent model to Equation 1 as a one-dimensional line integral where r is the distance to the hardbody perimeter and θ is the covariance-centric angular position measured from the x-axis. The probability density is symmetrized enabling the two-dimensional integral to be reduced to a one-dimensional path integral, resulting in the expression

$$P = \frac{-1}{2 \cdot \pi} \oint_{\text{ellipse}} \exp(-\alpha \cdot r^2) d\theta \quad (4a)$$

if the miss distance exceeds the combined object radius and

$$P = 1 - \frac{1}{2 \cdot \pi} \oint_{\text{ellipse}} \exp(-\alpha \cdot r^2) d\theta \quad (4b)$$

if the combined object radius exceeds the miss distance. Computation of the α term and Equation 4's numerical implementation involves coordinate rotation, scaling, and trigonometric functions as explained in Patera's paper. The method based on Reference 3 is currently employed in The Aerospace Corporation's Collision Vision Tool and Satellite Orbit Analysis Program (SOAP). The method is also used by various government and civil organizations.

B. Numerical testing

This 2001 covariance-centric method was programmed in FORTRAN with the number of integration steps (n) set to 400 as suggested by Patera. During testing, when the aspect ratio exceeded 50, some results were inside the operational decision making region. This was simply resolved by increasing the number of steps.

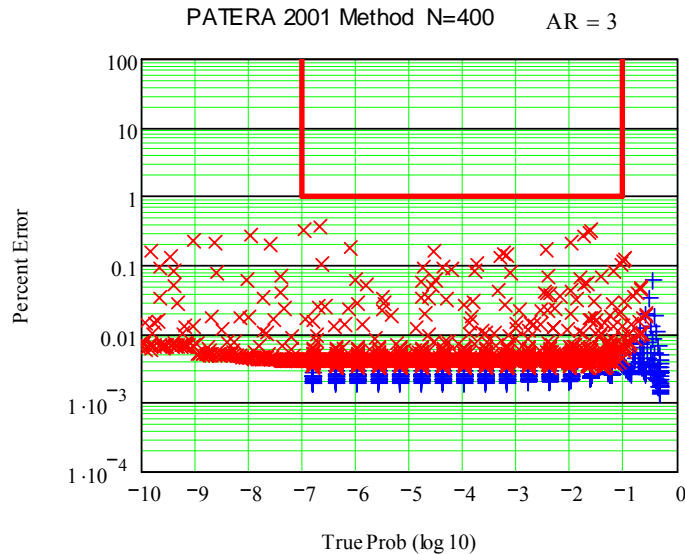


Figure 6a. Patera 2001 method (n=400) comparison with object smaller than or equal to miss distance

A complete set of 2001 case results can be found in Appendix A.

In a subsequent 2005 Engineering Note⁷ Patera switched the integration variable such that it was centered on the object. This change eliminated the trigonometric functions and also resulted in substantially fewer integration steps to achieve a given level of accuracy. This improved, object-centric method was programmed in FORTRAN. It produced better results and did so more quickly. The number of integration steps (n) was set to 50 as determined by numerous trials to prevent incursions into the operational decision making region.

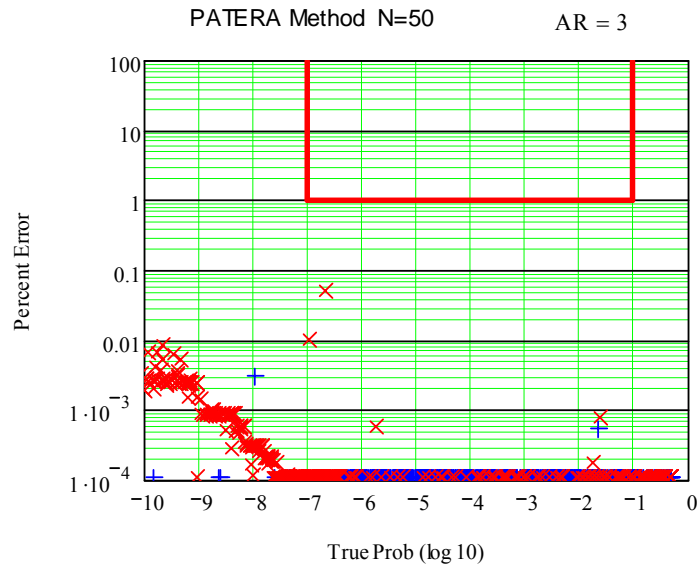


Figure 6b. Patera 2005 method (n=50) comparison with object smaller than or equal to miss distance

A complete set of 2005 case results can be found in Appendix B.

VI. Alfano's Method

A. General Method

Alfano⁴ developed a series expression to represent Equation 1 as a combination of error (erf) functions and exponential terms. In the encounter plane, the combined object center's location is (x_m, y_m) with associated standard deviations σ_x and σ_y and combined object radius OBJ. The series expression is given as

$$P = \frac{OBJ \cdot 2}{\sqrt{8 \cdot \pi \cdot \sigma_x \cdot n}} \cdot \sum_{i=0}^n \left[\operatorname{erf} \left[\frac{\left[y_m + \frac{2 \cdot OBJ}{n} \cdot \sqrt{(n-i) \cdot i} \right]}{(\sigma_y \cdot \sqrt{2})} \right] + \operatorname{erf} \left[\frac{\left[-y_m + \frac{2 \cdot OBJ}{n} \cdot \sqrt{(n-i) \cdot i} \right]}{(\sigma_y \cdot \sqrt{2})} \right] \right] \cdot \exp \left[\frac{\left[\frac{OBJ \cdot (2 \cdot i - n)}{n} + x_m \right]^2}{2 \cdot \sigma_x^2} \right] \quad (5a)$$

The method then breaks the series into m-even and m-odd components and makes use of Simpson's one-third rule. An expression to determine a sufficiently small number of terms is given as

$$m = \operatorname{int} \left(\frac{5 \cdot OBJ}{\min(\sigma_x, \sigma_y, \sqrt{x_m^2 + y_m^2})} \right) \quad (5b)$$

with a lower bound of 10 and upper bound of 50. This method is currently implemented in Analytical Graphics, Inc., Satellite Tool Kit.

B. Numerical testing

Equations 5a and 5b were programmed in FORTRAN. No results appeared inside the operational decision making region for any of the test cases because of the sufficiency of Equation 5b. Greater accuracy, if desired, can be achieved by increasing m.

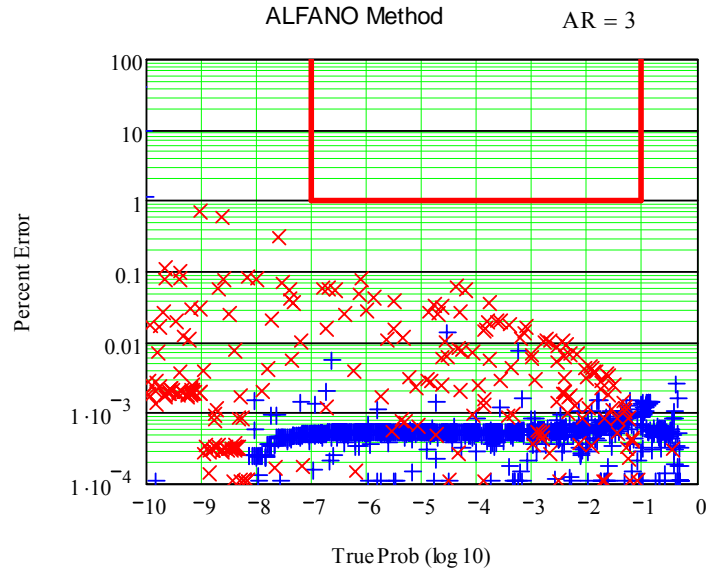


Figure 7. Alfano method comparison with object smaller than or equal to miss distance

A complete set of case results can be found in Appendix A.

VII. Practical Considerations

Within the bounds of testing and observed limits, all four methods are sufficiently accurate for analysis of satellite conjunctions. Chan's method is by far the fastest but is also the most restrictive due to relative object size limitations. Patera's method produces good results, especially with his more-recent object-oriented formulation. Alfano's method determines the number of integrations steps on a case-by-case basis. Foster's method is the slowest, but can be sped up by increasing the step size for many cases without adversely affecting accuracy.

The operational decision-making region defined in this paper is only a suggestion. The user must decide what level of accuracy is required over a given range of probabilities. For trend analysis, speed might be more important than accuracy to a large number of decimal places. Accuracy will be the driver for maneuver decisions where fuel will be expended and on-orbit lifetime shortened. For co-orbiting satellites, the linear relative velocity assumption may be invalid. Whatever the purpose, the user must understand the limits and assumptions that apply to each method before choosing.

VIII. Conclusion

Four methods were reviewed for determining collision probability of spherical objects exhibiting linear relative motion. Testing was performed over a wide range of parameters and results were compared to a truth set accurate to at least 9 decimal places. An operational decision-making region was defined to further assess computational results. All four methods produced acceptable results within the bounds of testing and observed limits. These methods can be found in commercial and/or government tools.

Foster casts the problem in polar coordinates, then sections the object footprint into numerous radial and angular pieces to compute conjunction probability. Chan develops an analytical approximation by transforming the two-dimensional Gaussian probability density function (pdf) to a one-dimensional Rician pdf and uses the concept of equivalent areas. Patera symmetrizes the probability density to enable reduction to a one-dimensional line integral. Alfano uses error functions and exponential terms to develop a series expression that makes use of Simpson's one-third rule.

IX. Acknowledgements

I wish to thank Ken Chan, Eric George, Russ Patera, and Glenn Peterson, of the Aerospace Corporation, for reviewing this paper. Ken was instrumental in providing the technical details of implementation for several of the methods reviewed. He also shared some of the results from his upcoming book on this same subject. Russ assisted in assuring proper implementation of his method. I would also like to thank the Center for Space Standards and Innovation team (Dave Finkleman, T. S. Kelso, and Dave Vallado) for reviewing this paper and providing valuable comments.

References

¹Foster, J. L., and Estes, H. S., "A Parametric Analysis of Orbital Debris Collision Probability and Maneuver Rate for Space Vehicles," NASA/JSC-25898, August 1992.

²Chan, K., "Collision Probability Analyses for Earth-Orbiting Satellites," Proceedings of the 7th International Space Conference of Pacific Basin Societies, Nagasaki, Japan, July 1997.

³Patera, R. P. "General Method for Calculating Satellite Collision Probability," *Journal of Guidance, Control, and Dynamics*, Vol. 24, No. 4, July-August 2001, pp. 716-722.

⁴Alfano, S. "A Numerical Implementation of Spherical Object Collision Probability," *Journal of the Astronautical Sciences*, Vol. 53, No. 1, January-March 2005, pp. 103-109.

⁵Chan, K., "Short-Term vs Long-Term Spacecraft Encounters," AIAA Paper No. 2004-5460, AIAA/AAS Astrodynamics Specialist Conference, Providence, Rhode Island, 16-19 August, 2004.

⁶Chan, K., "Improved Analytical Expressions for Computing Spacecraft Collision Probabilities," AAS Paper No. 03-184, AAS/AIAA Space Flight Mechanics Meeting, Ponce, Puerto Rico, 9-13 February 2003.

⁷Patera, R. P. "Calculating Collision Probability for Arbitrary Space-Vehicle Shapes via Numerical Quadrature," *Journal of Guidance, Control, and Dynamics*, Vol. 28, No. 6, November-December 2005, pp. 1326-1328.

Appendix A

Foster method unfiltered results

Chan method unfiltered results

Patera 2001 method results

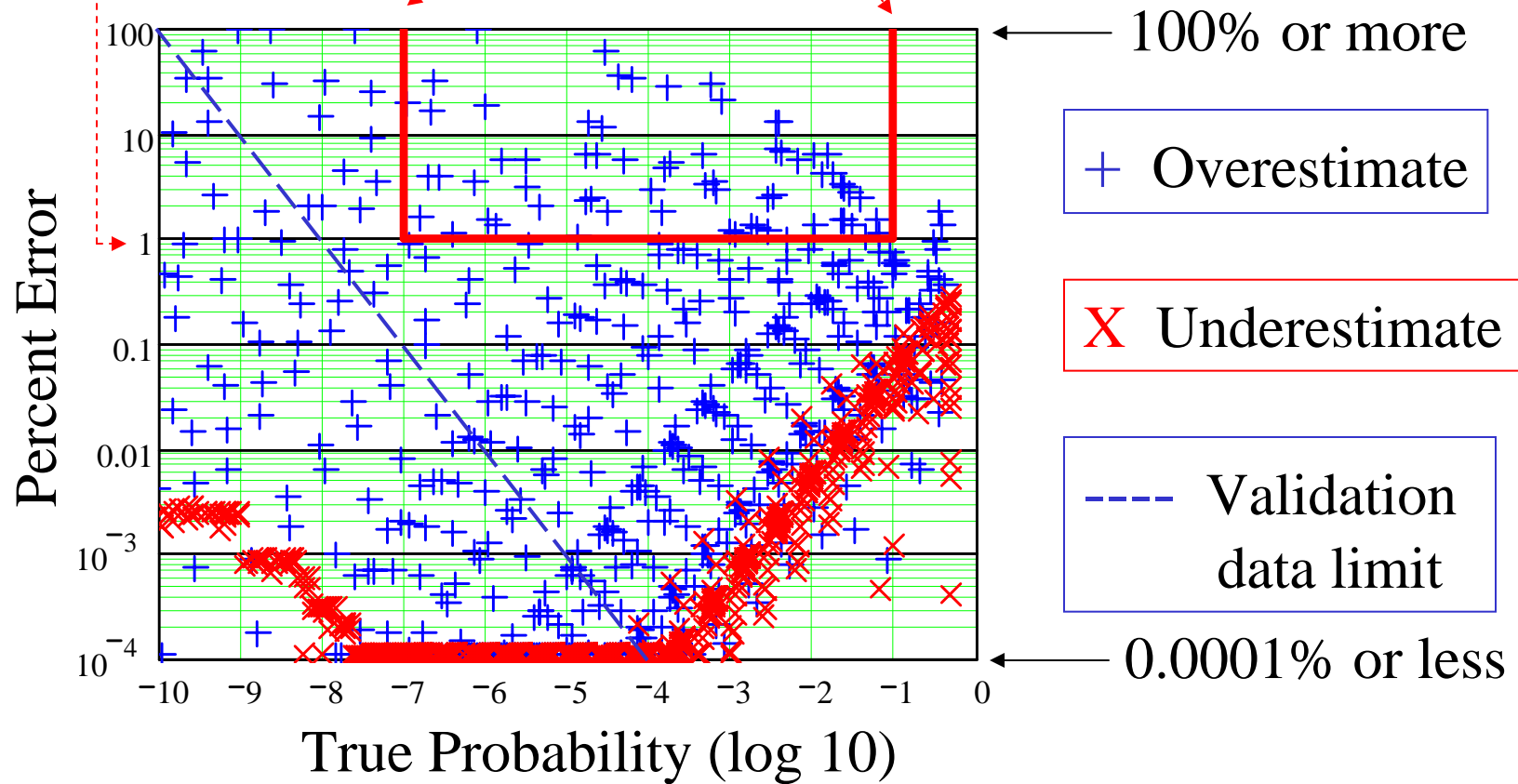
Alfano method results

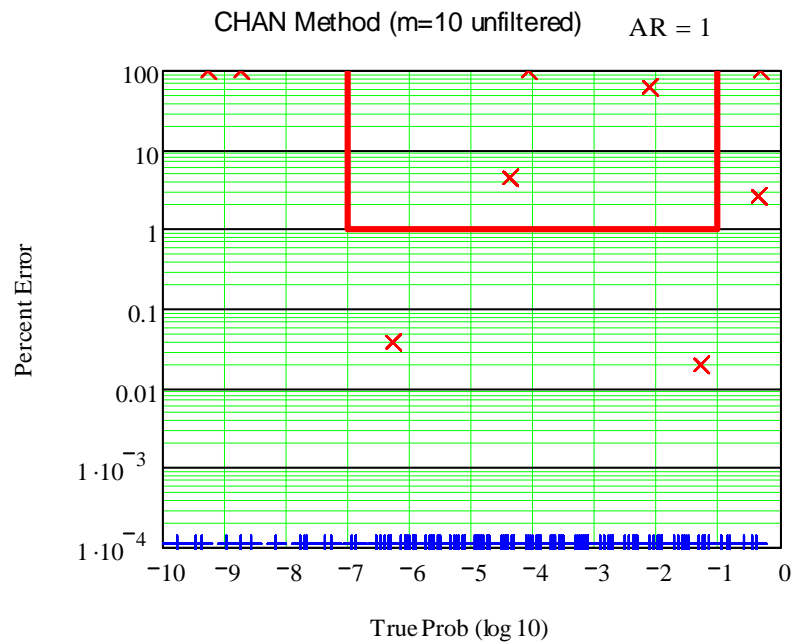
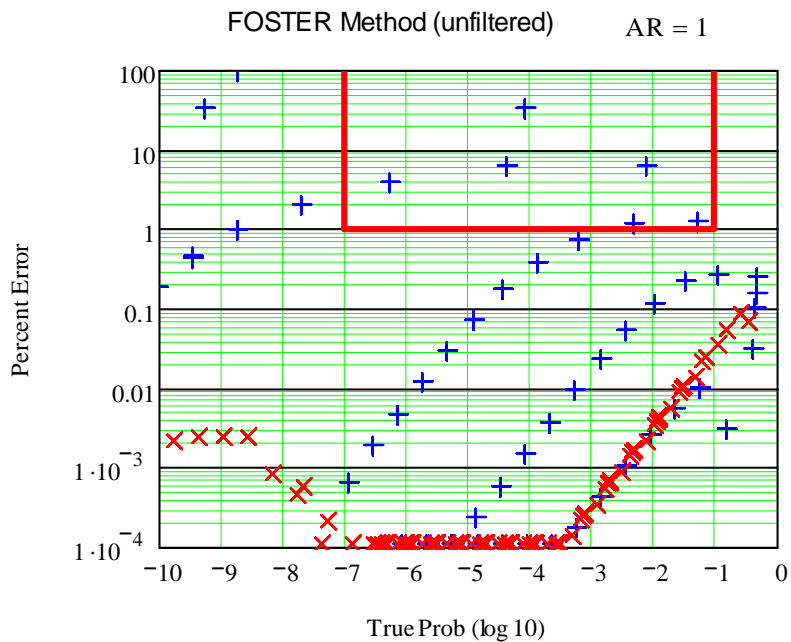
Legend

Slide layout	
FOSTER	CHAN
PATERA	ALFANO

Operational decision making region

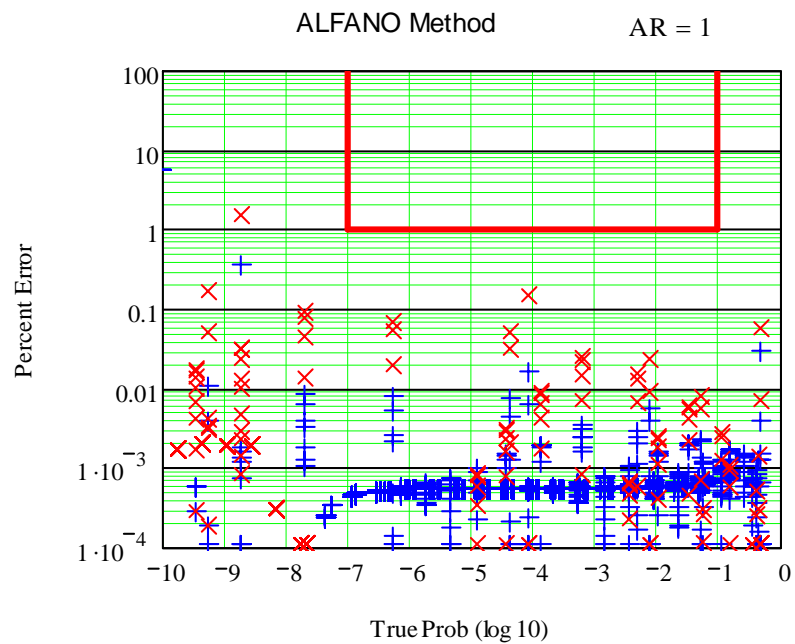
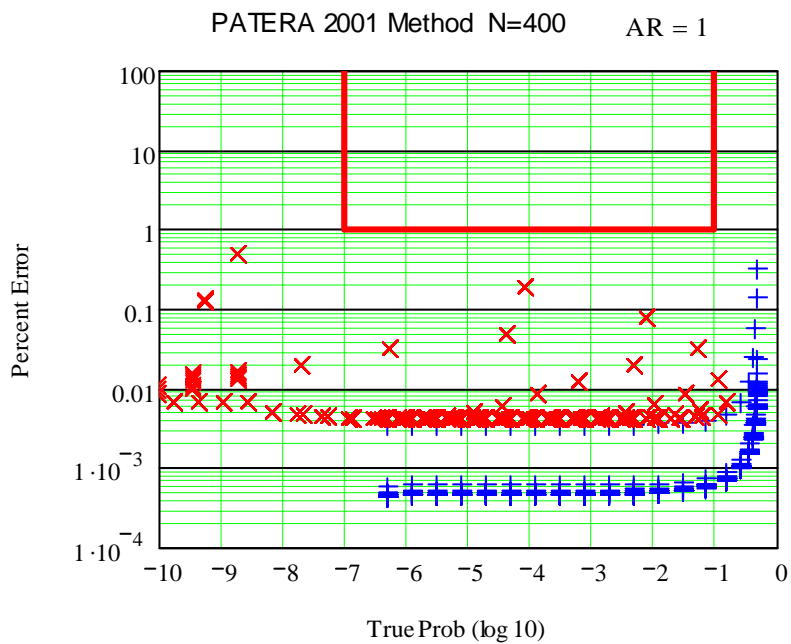
1% error for $10^{-7} < P < 10^{-1}$

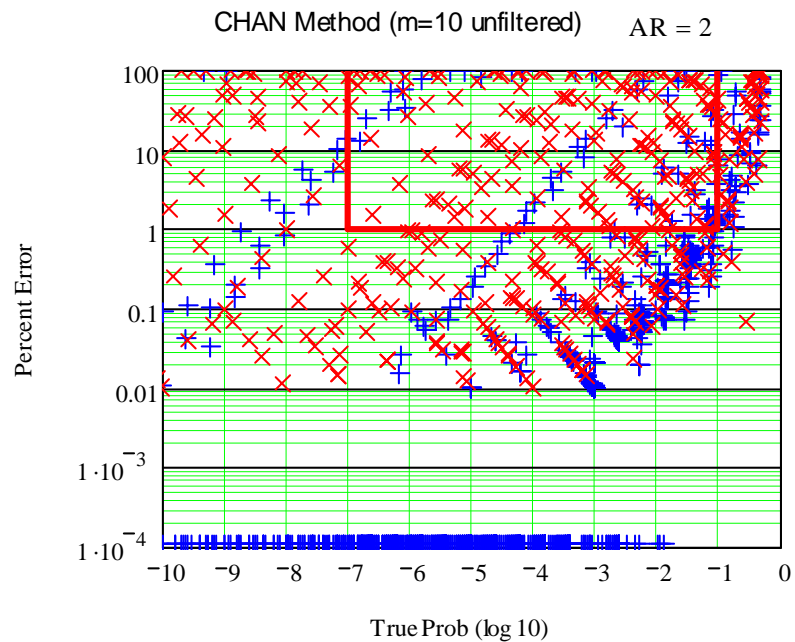
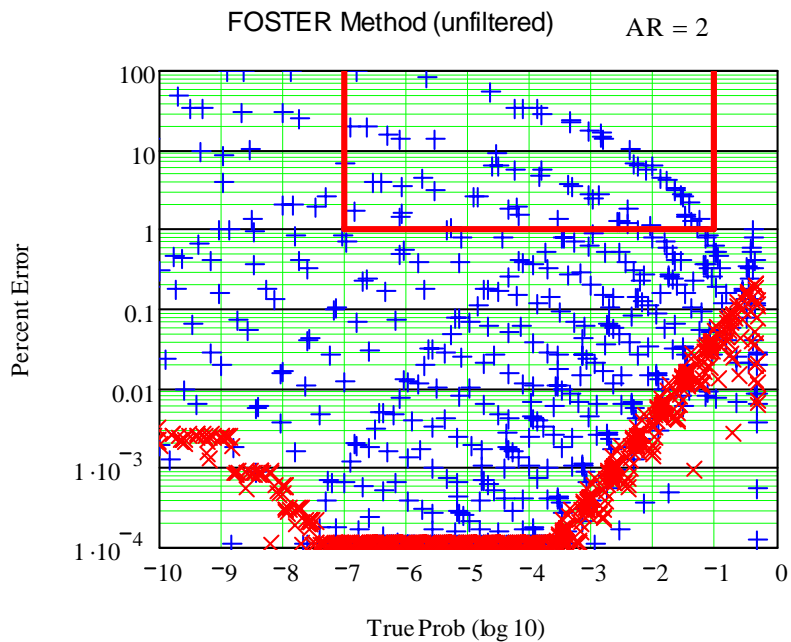




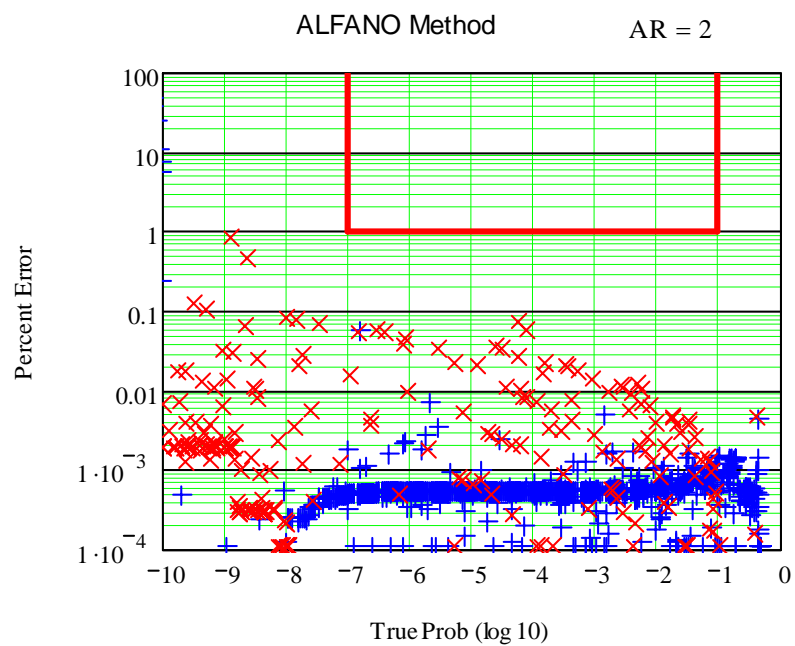
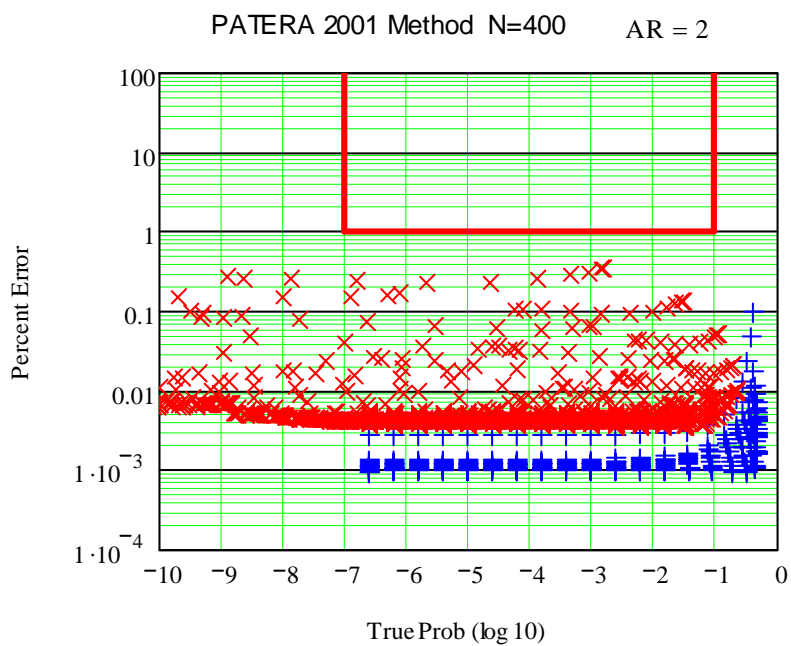
OBJ \leq DIST

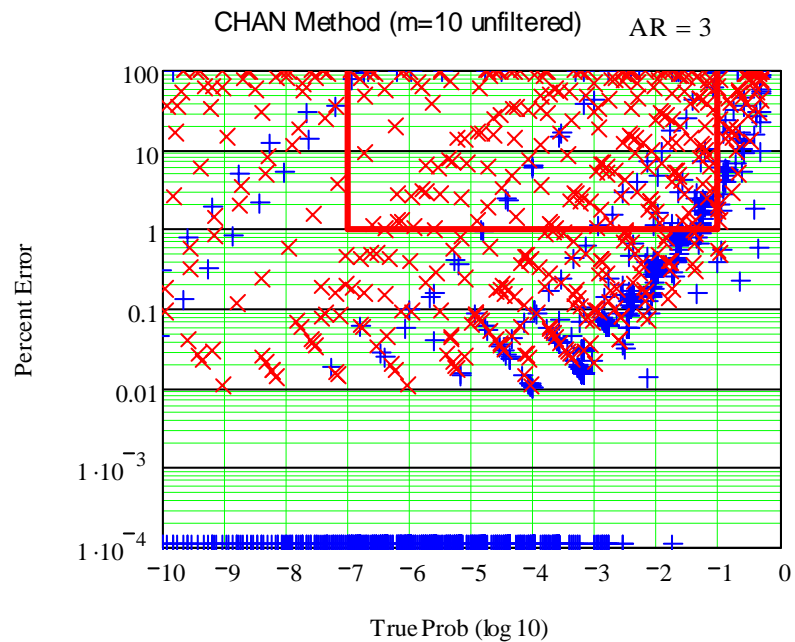
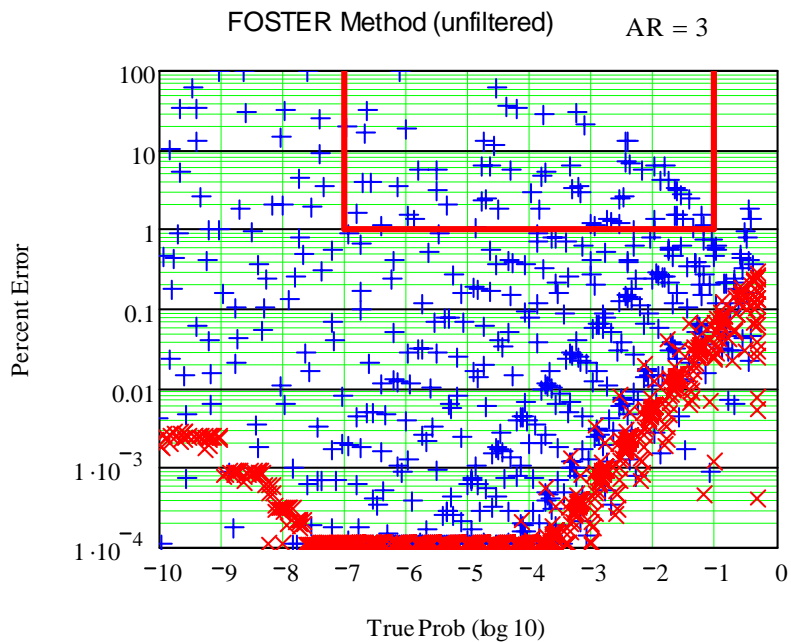
AR=1



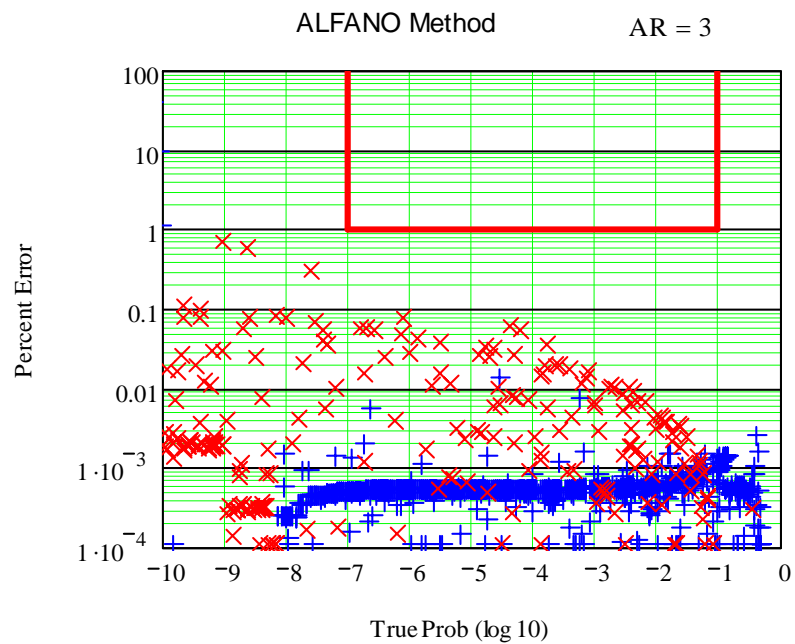
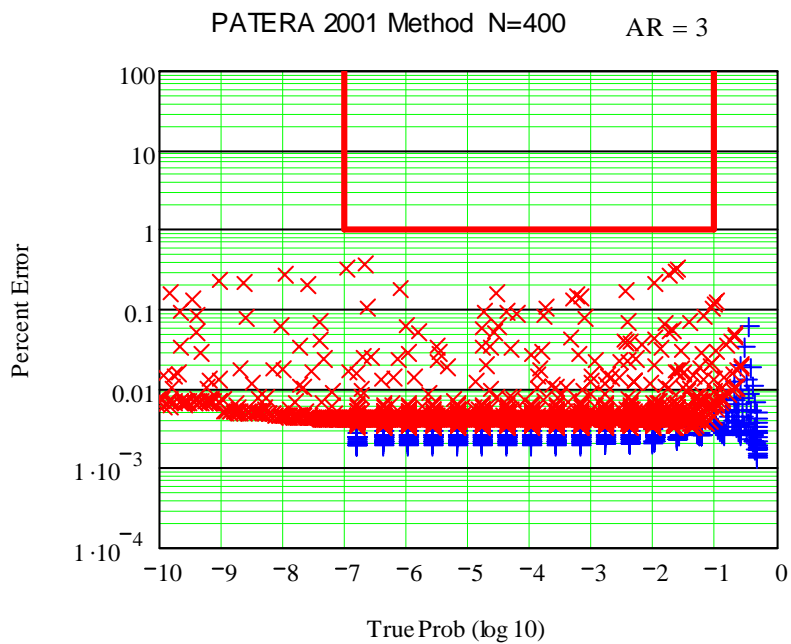


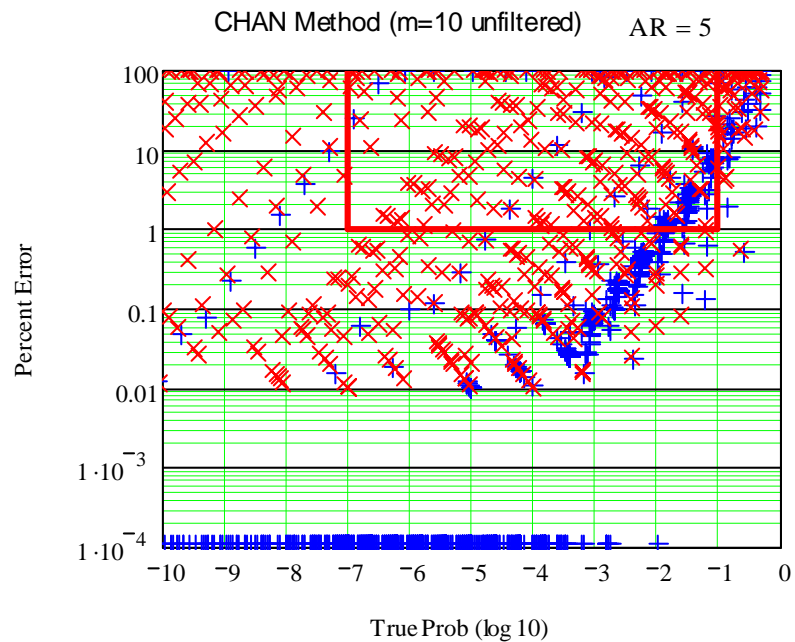
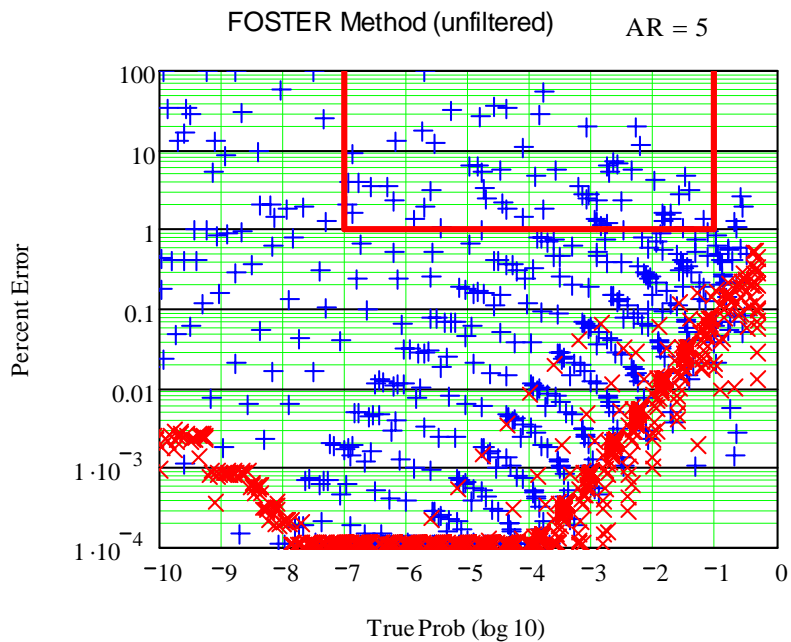
OBJ \leq DIST AR=2



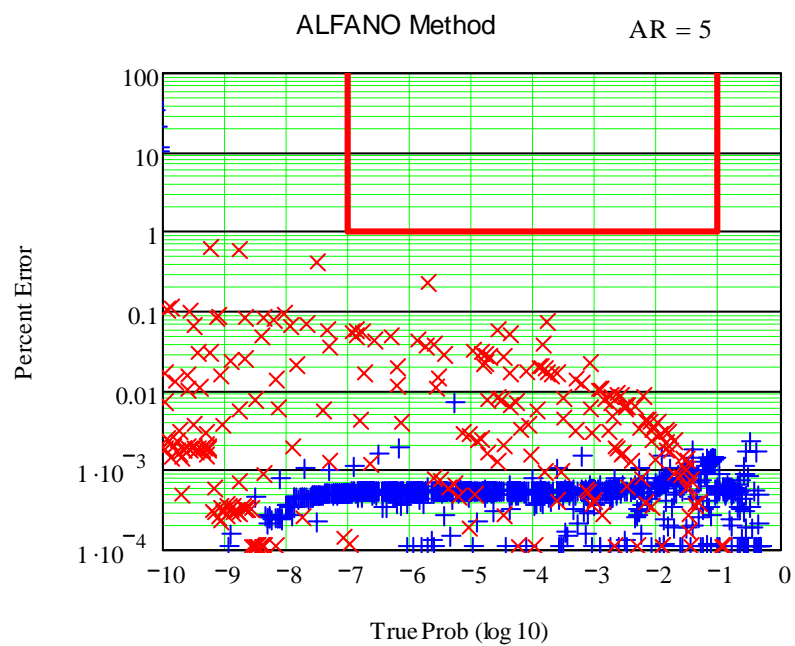
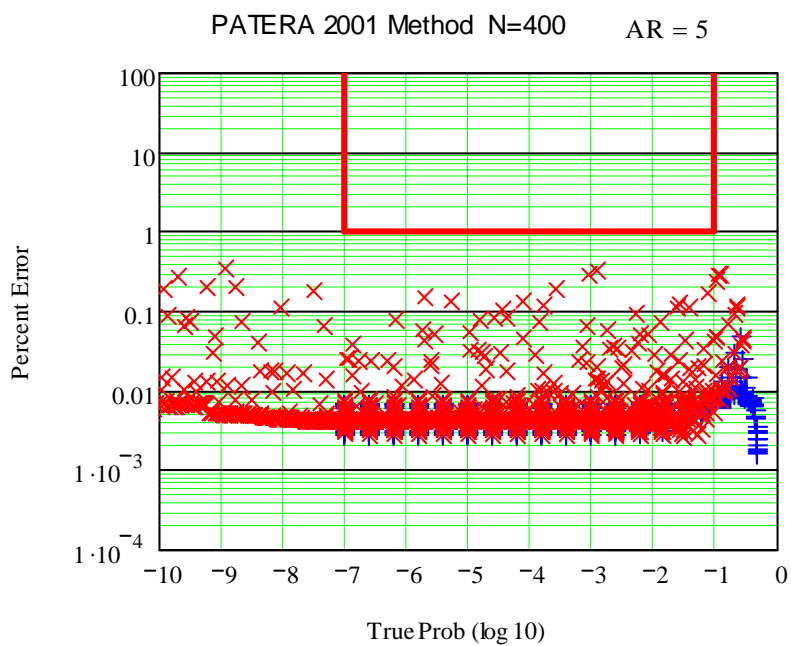


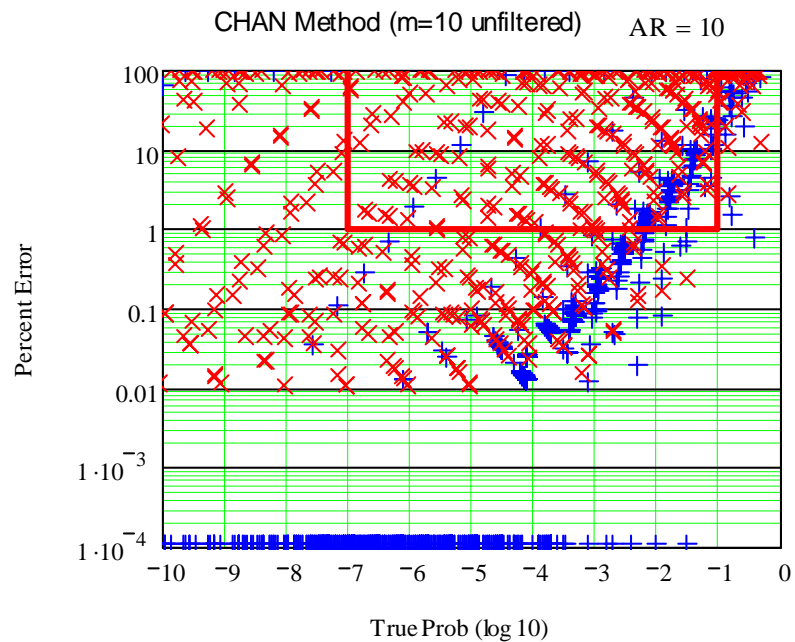
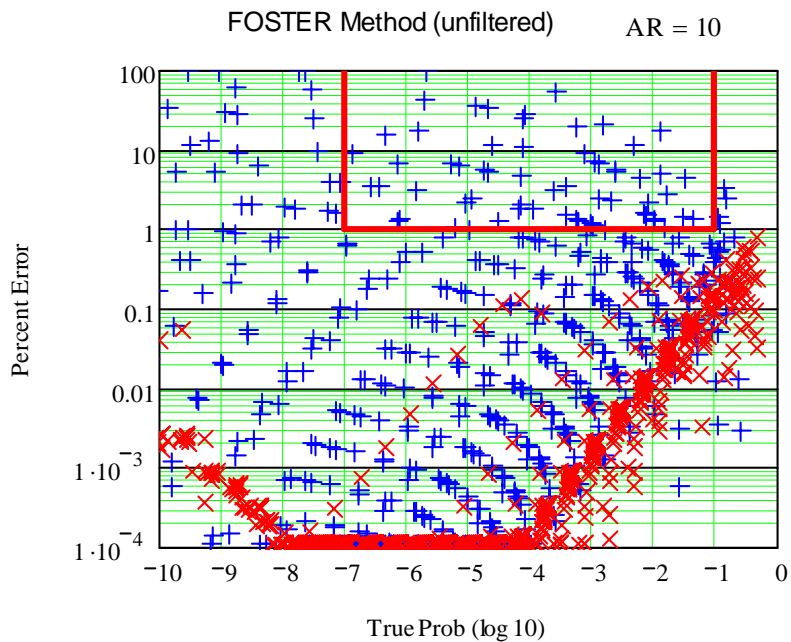
OBJ \leq DIST AR=3



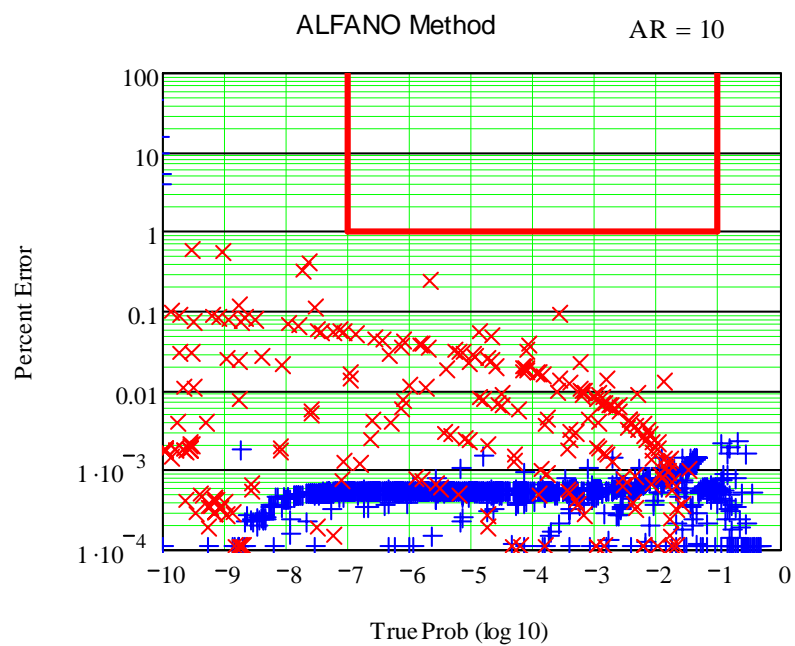
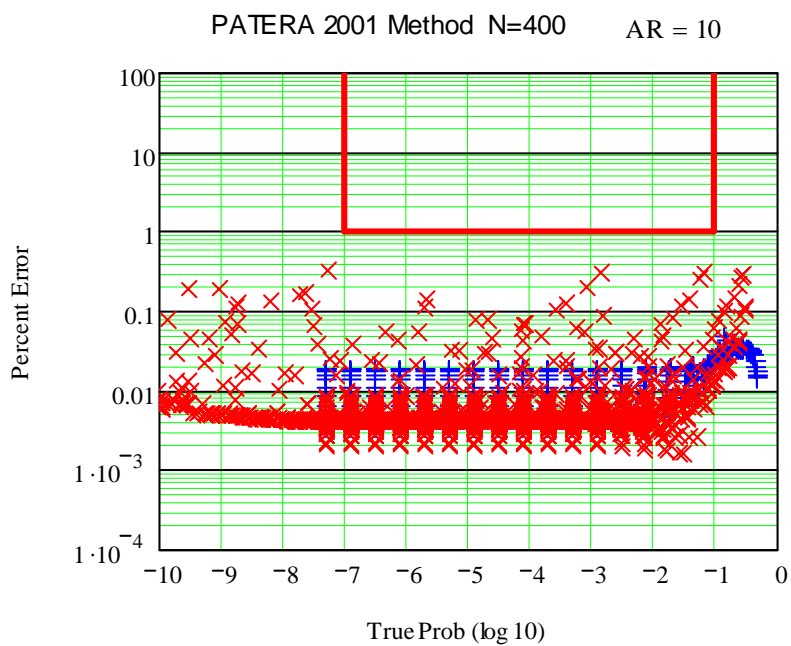


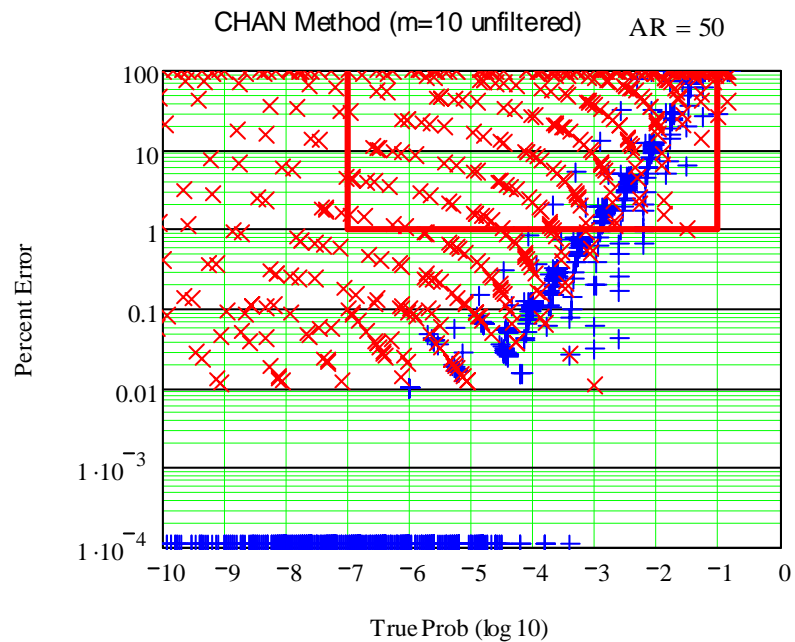
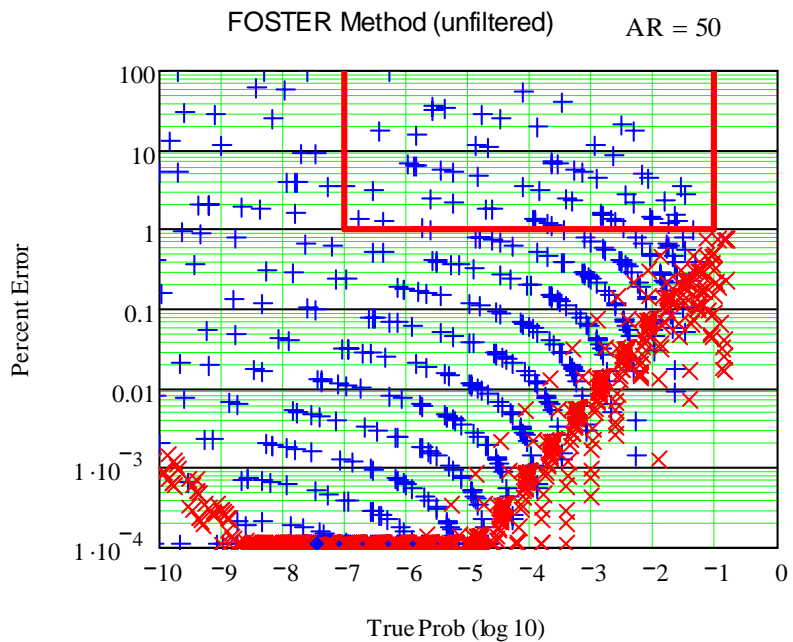
OBJ \leq DIST AR=5



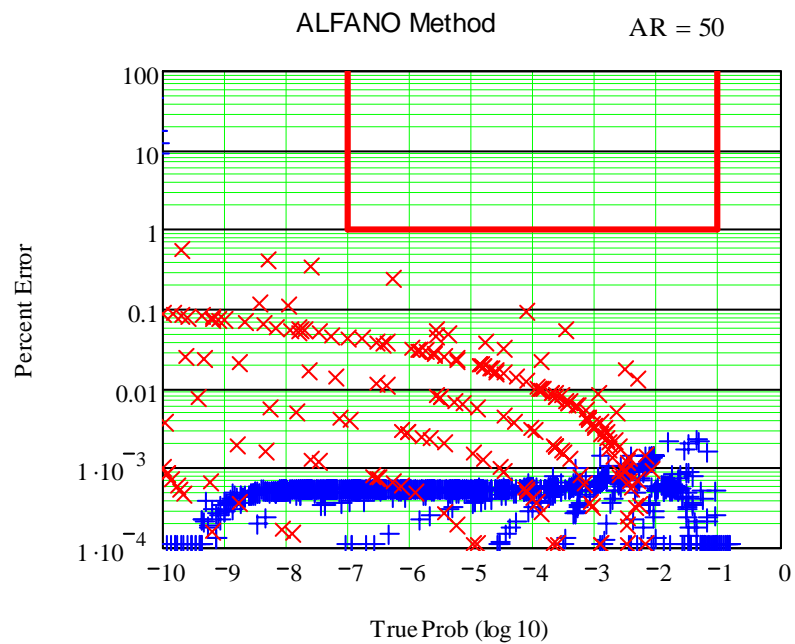
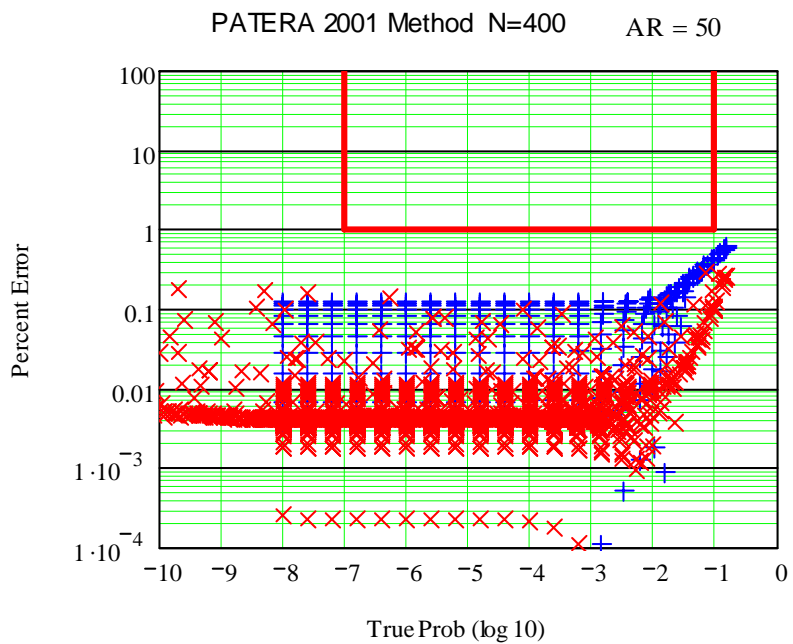


OBJ \leq DIST AR=10

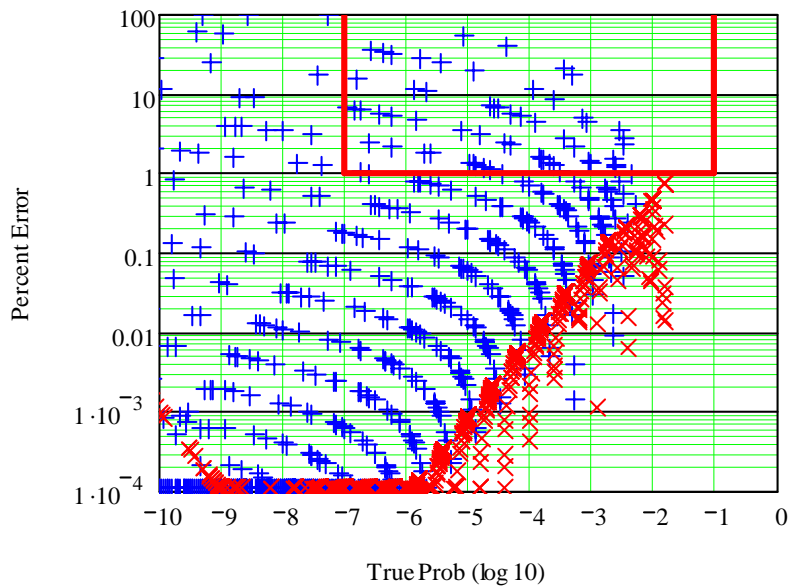




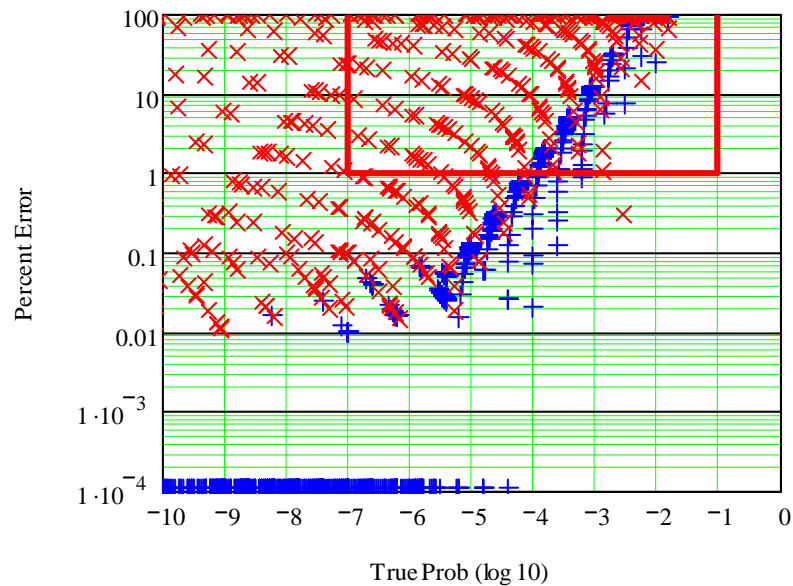
OBJ \leq DIST AR=50



FOSTER Method (unfiltered) AR = 500

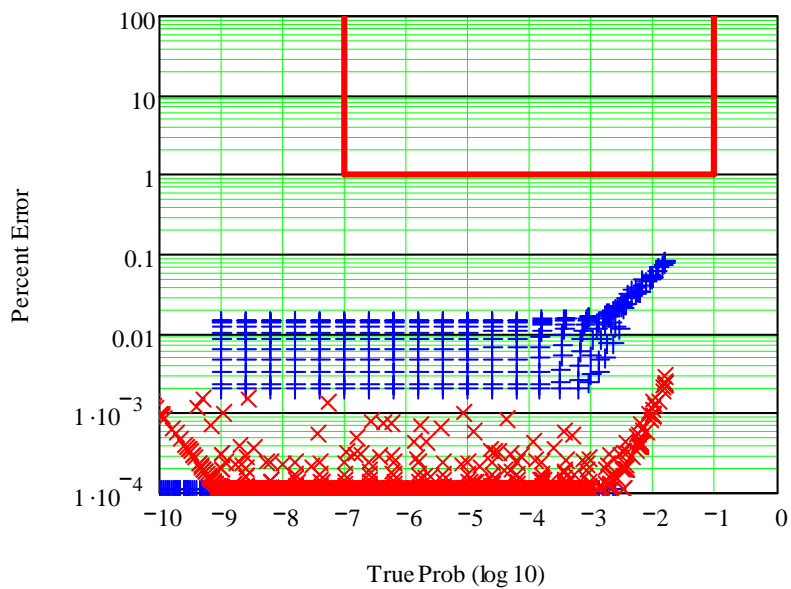


CHAN Method (m=10 unfiltered) AR = 500

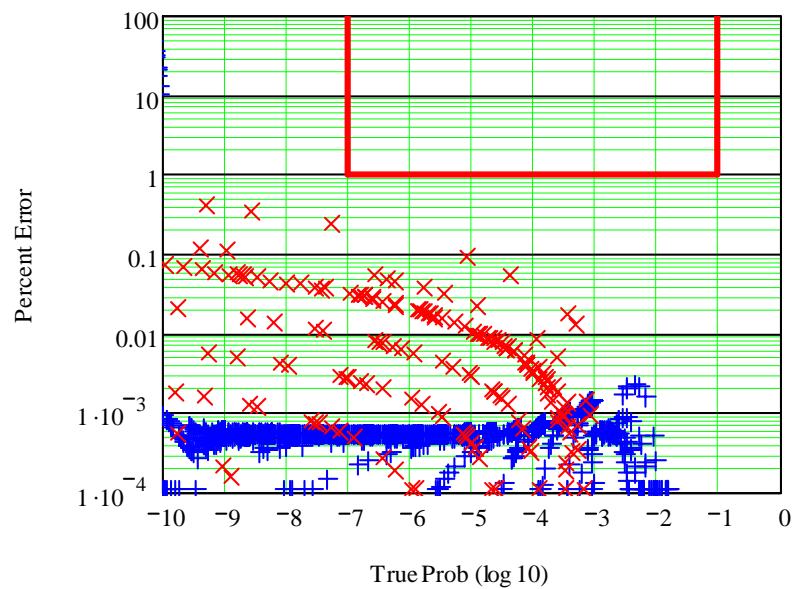


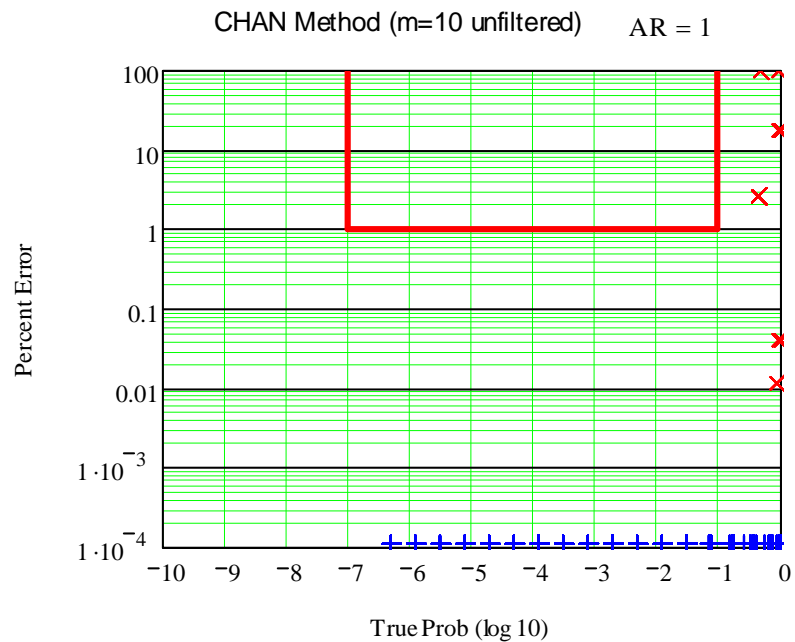
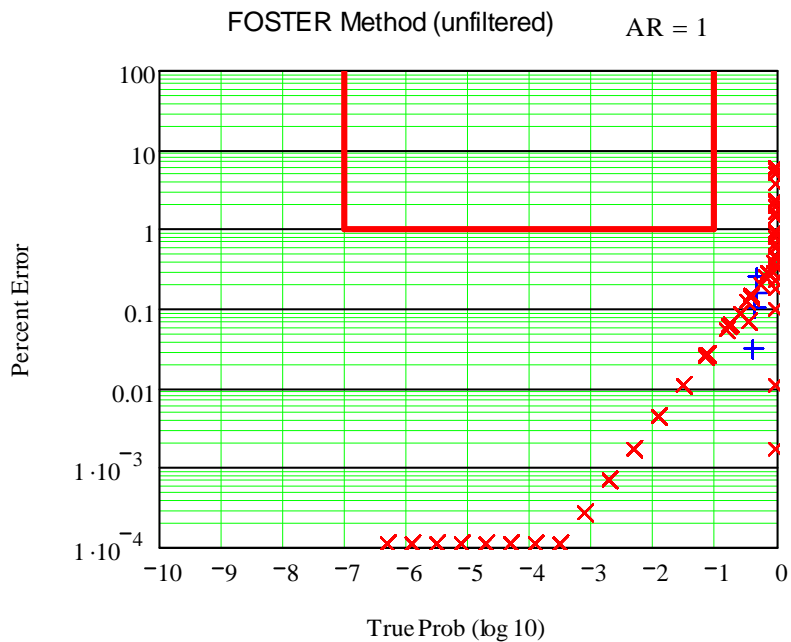
OBJ <= DIST AR=500

PATERA 2001 Method N=4000 AR = 500



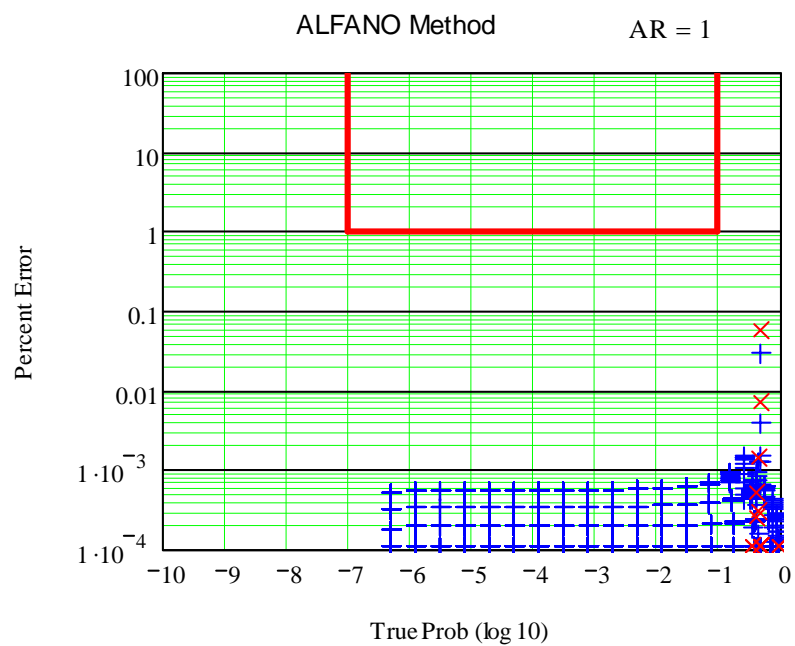
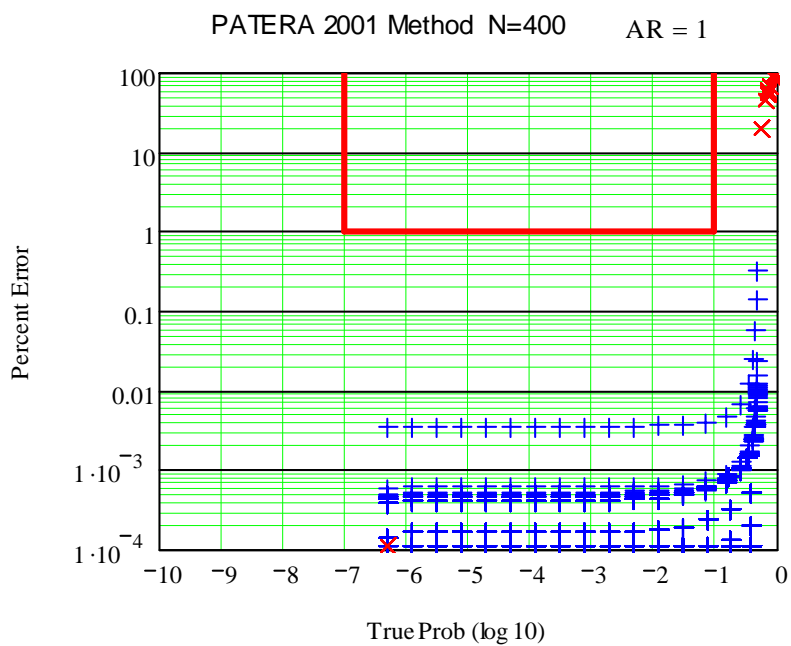
ALFANO Method AR = 500

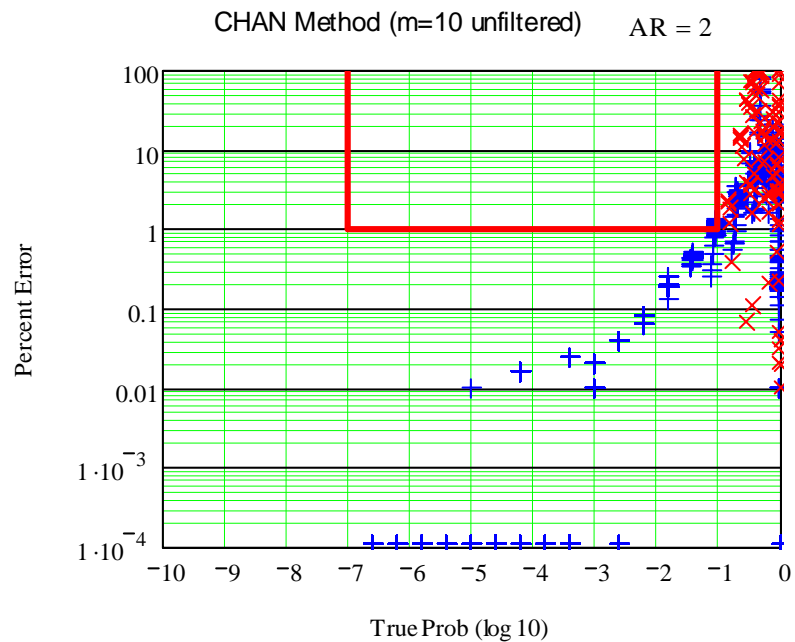
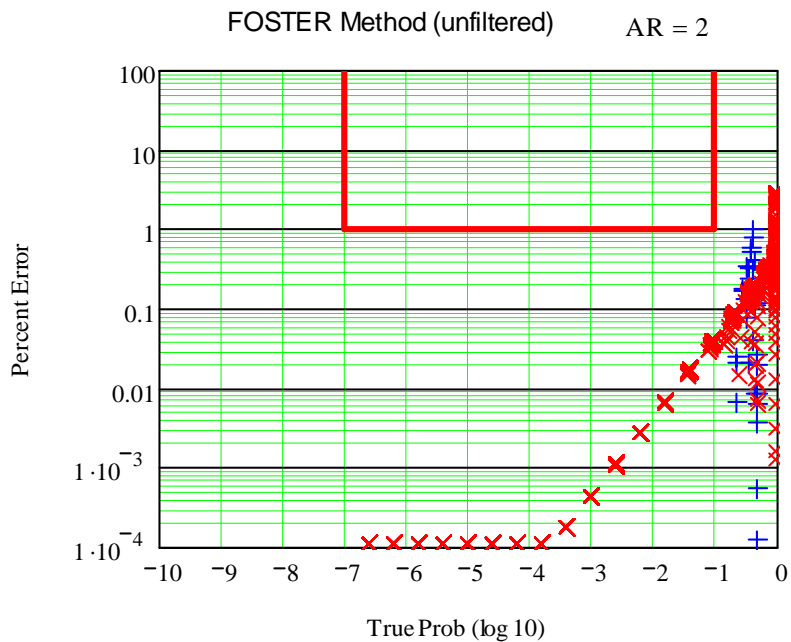




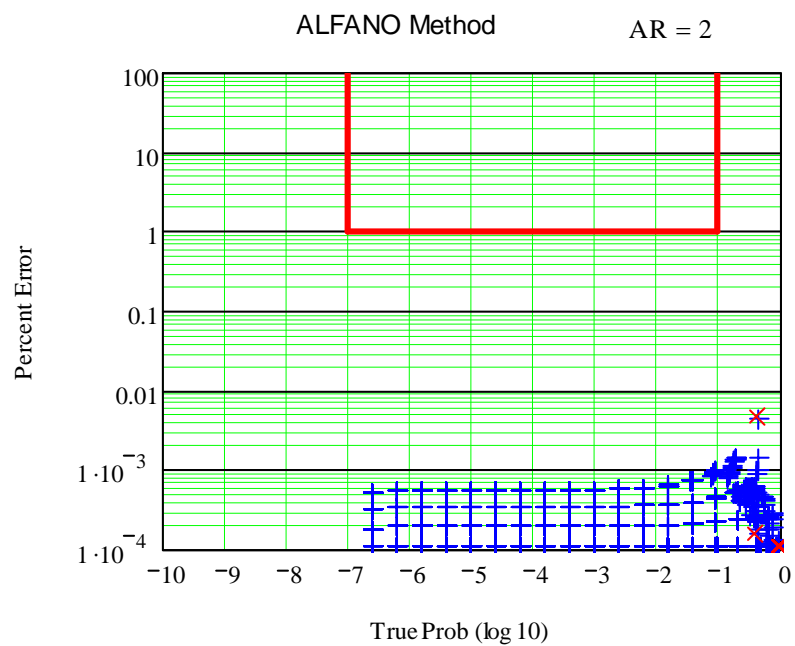
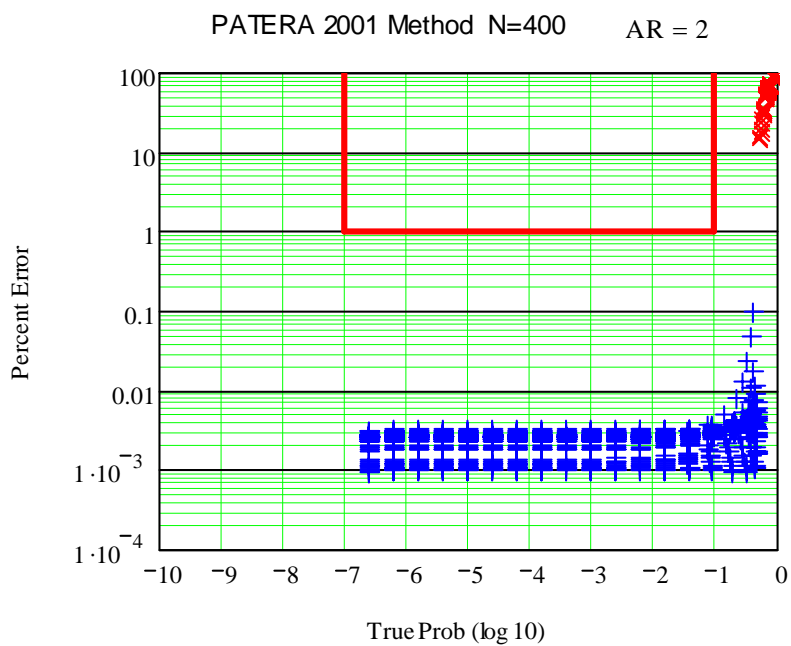
OBJ > DIST

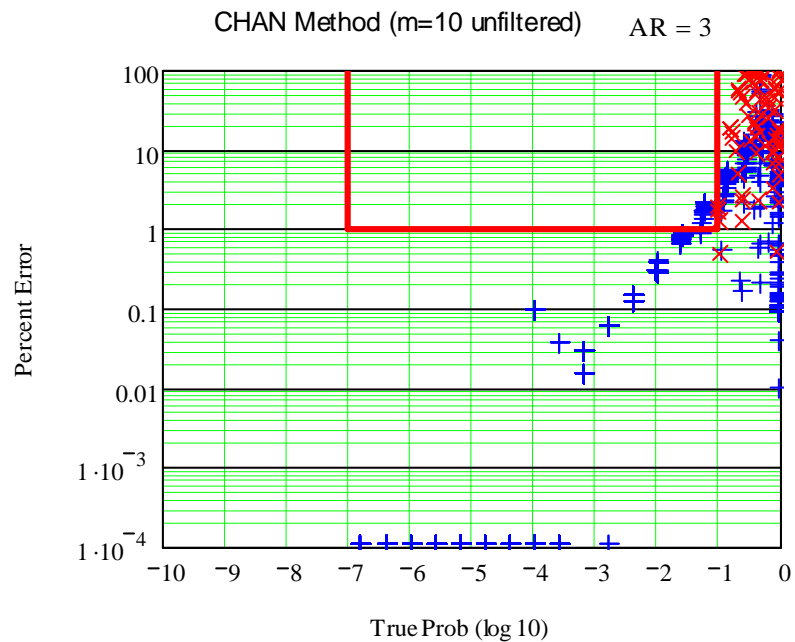
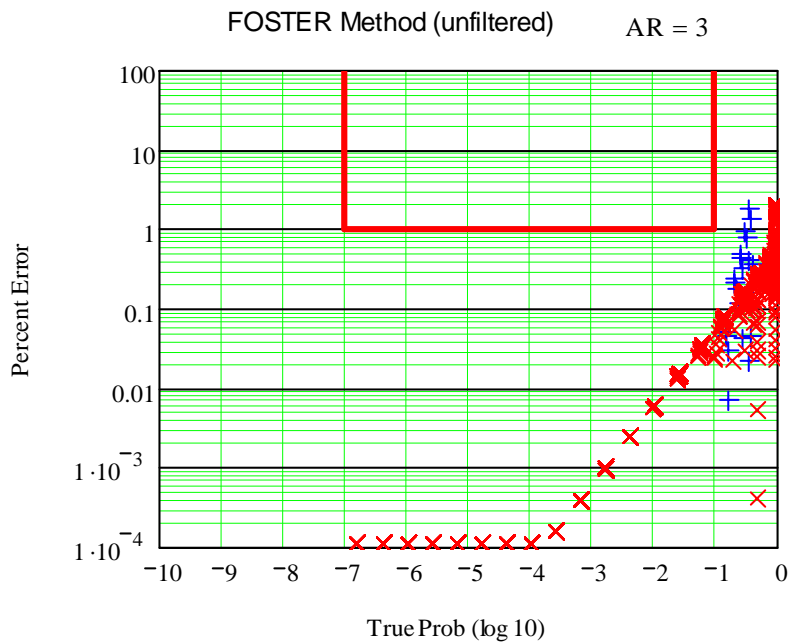
AR=1



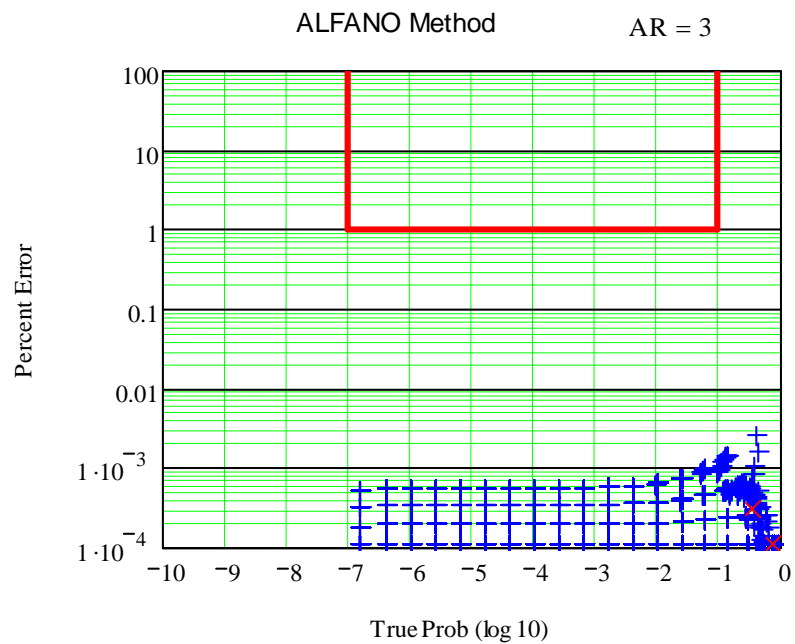
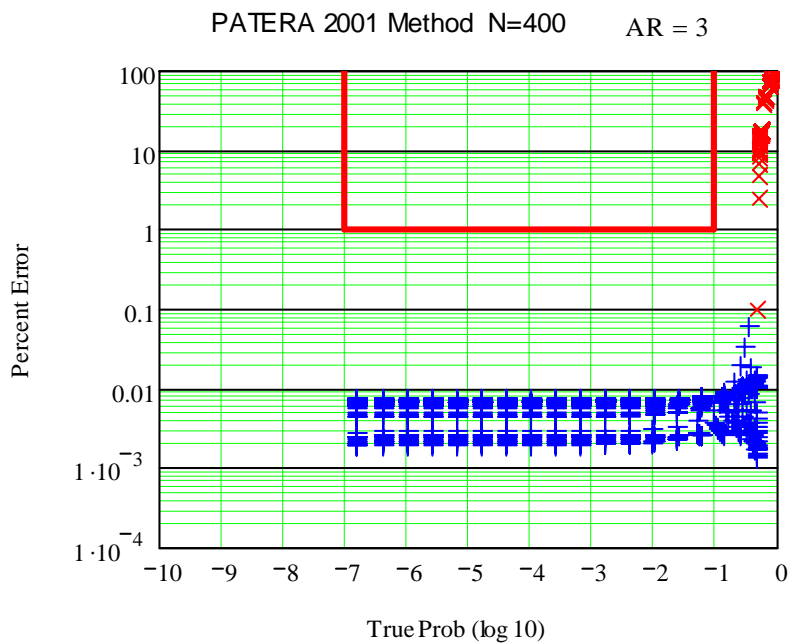


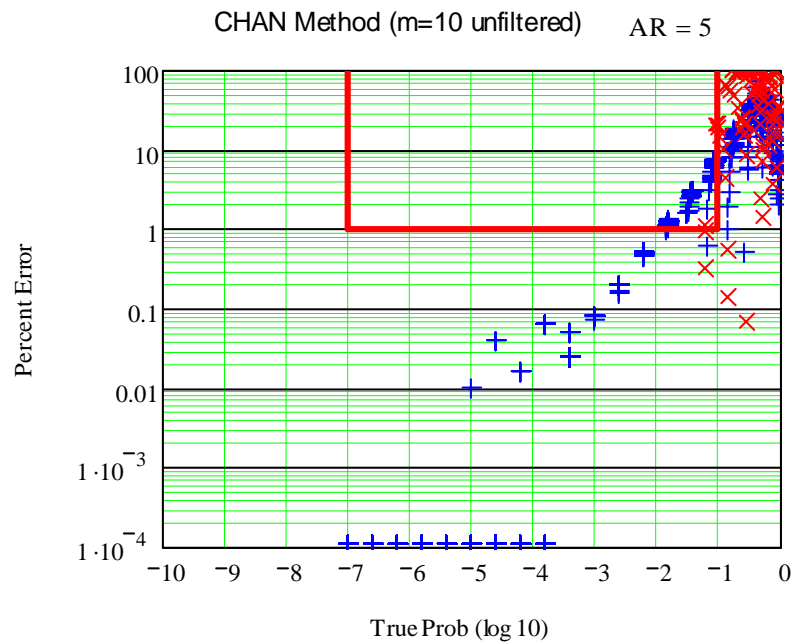
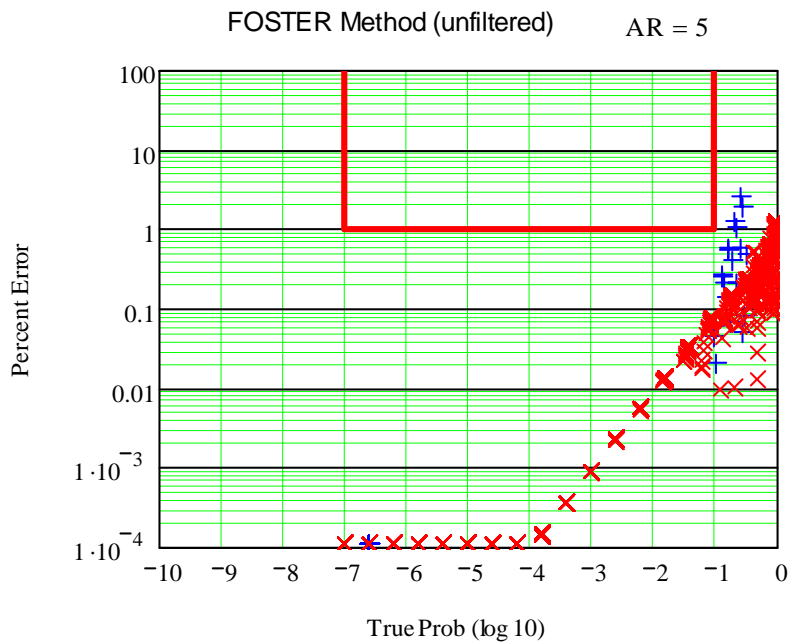
OBJ > DIST AR=2



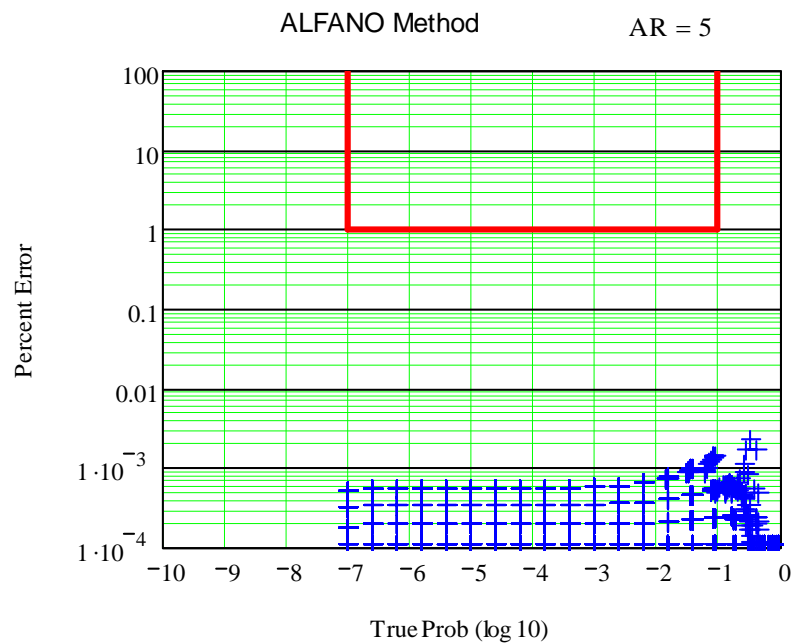
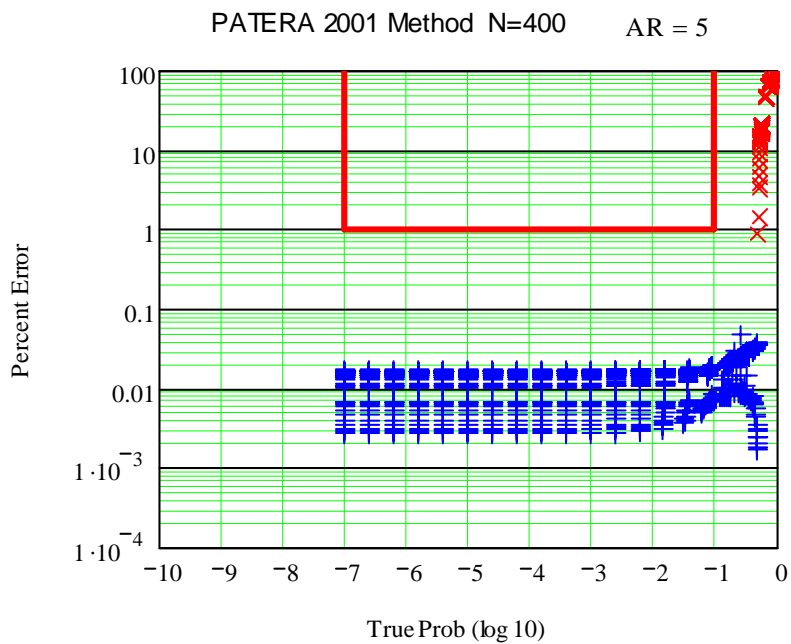


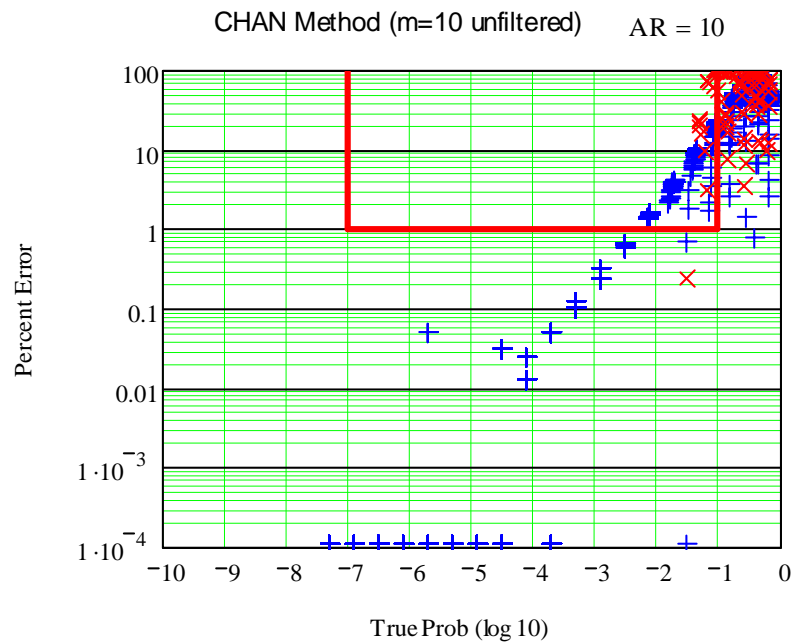
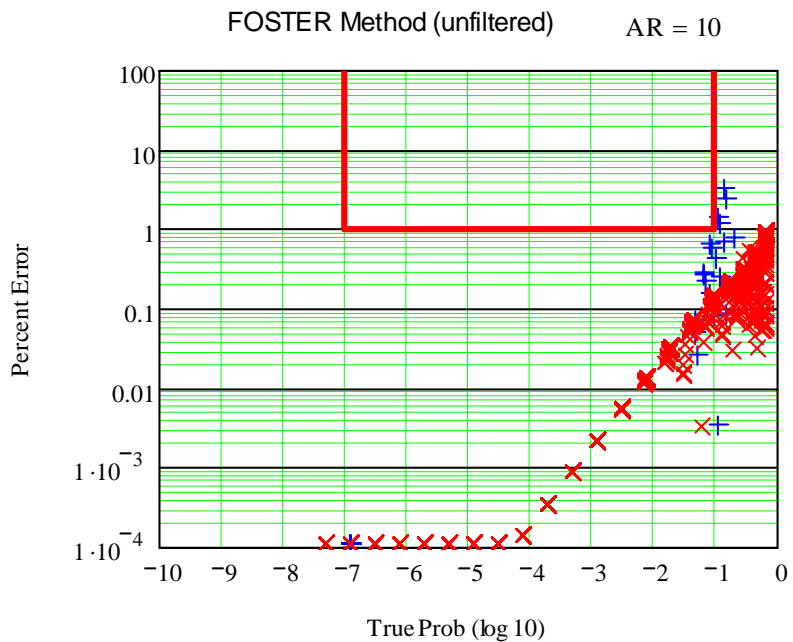
OBJ > DIST AR=3



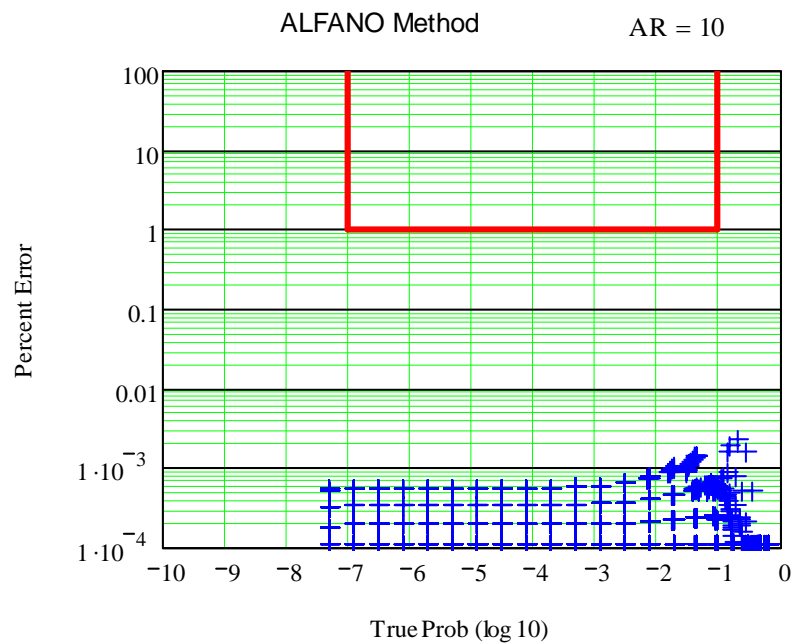
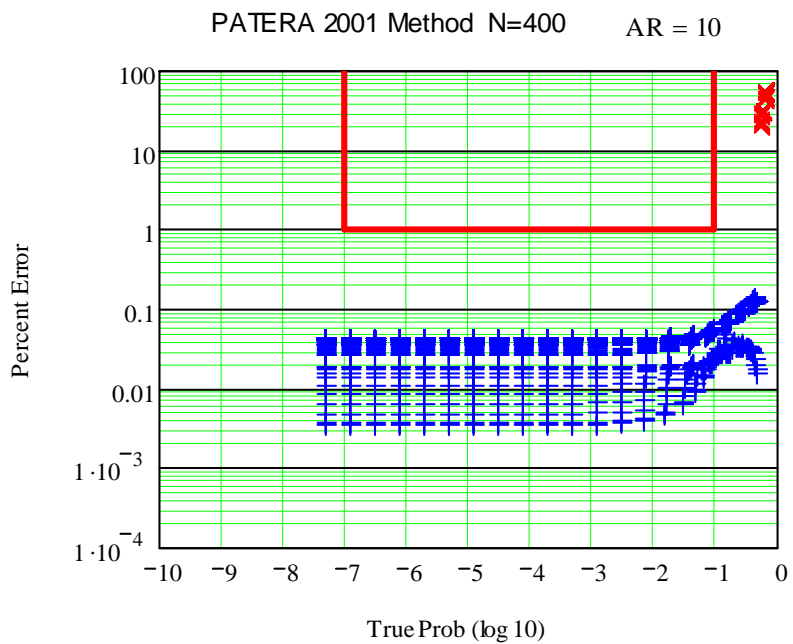


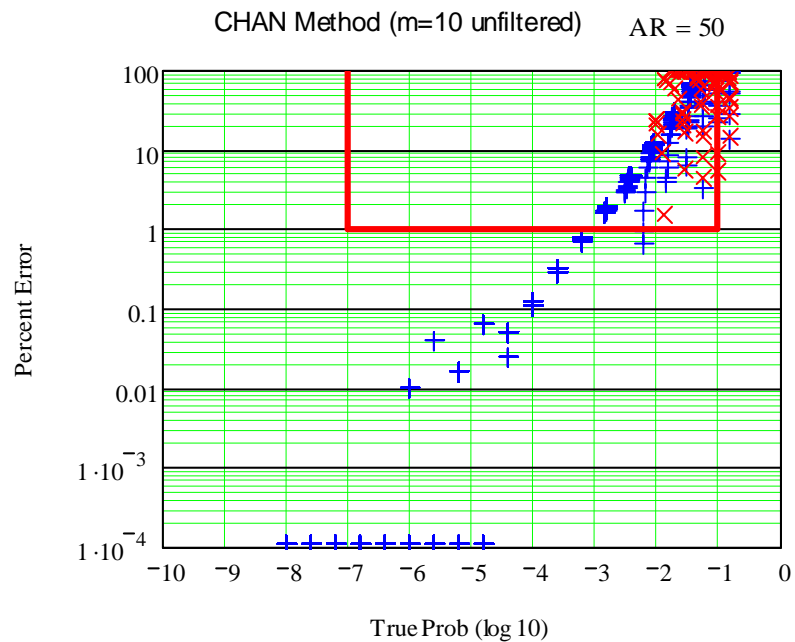
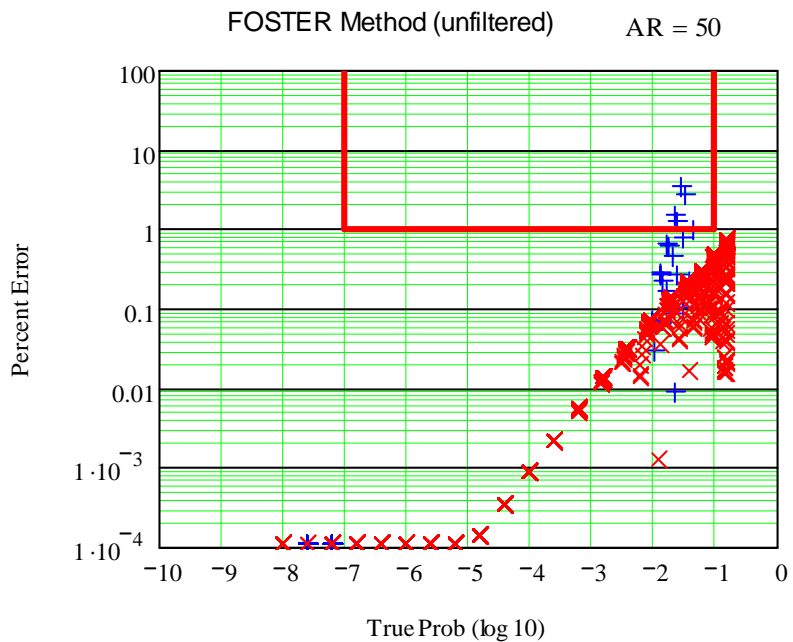
OBJ > DIST AR=5



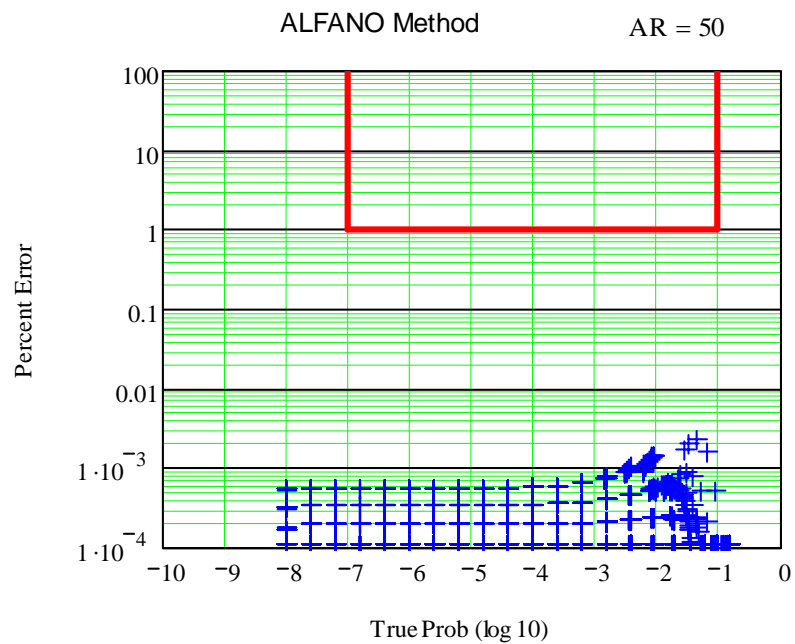
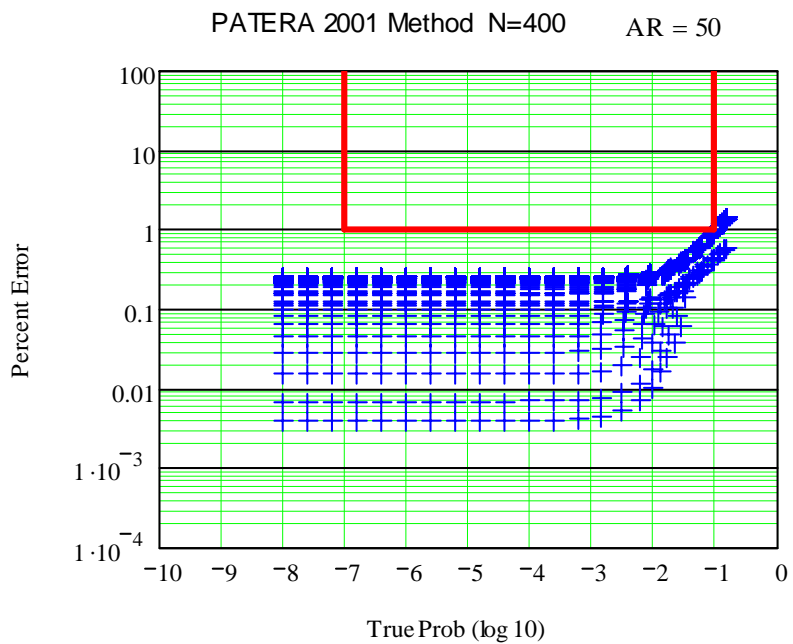


OBJ > DIST AR=10

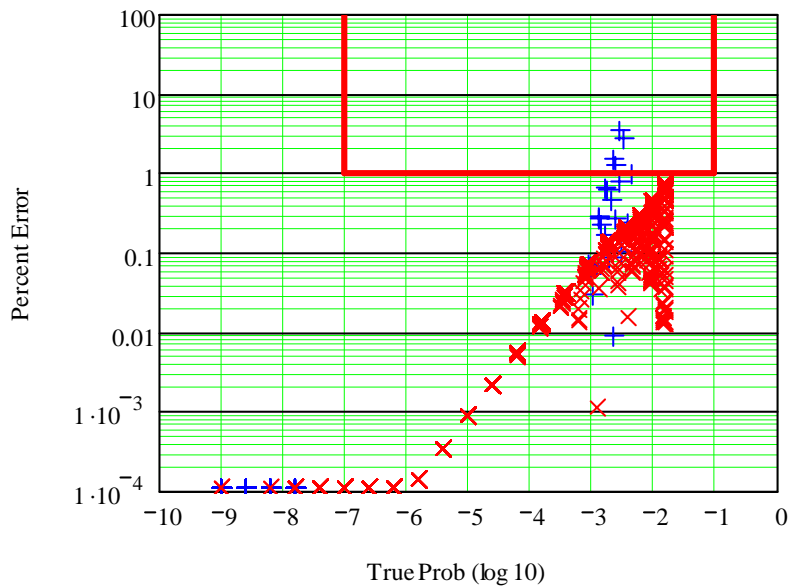




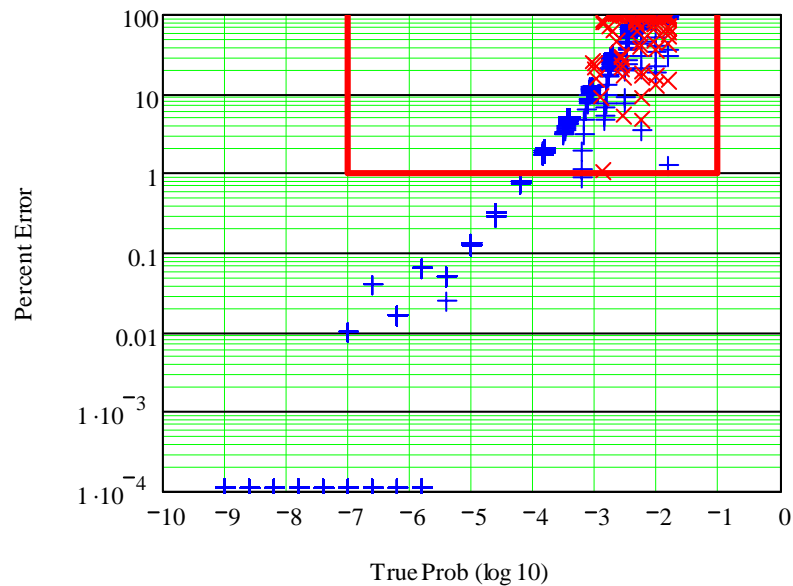
OBJ > DIST AR=50



FOSTER Method (unfiltered) AR = 500

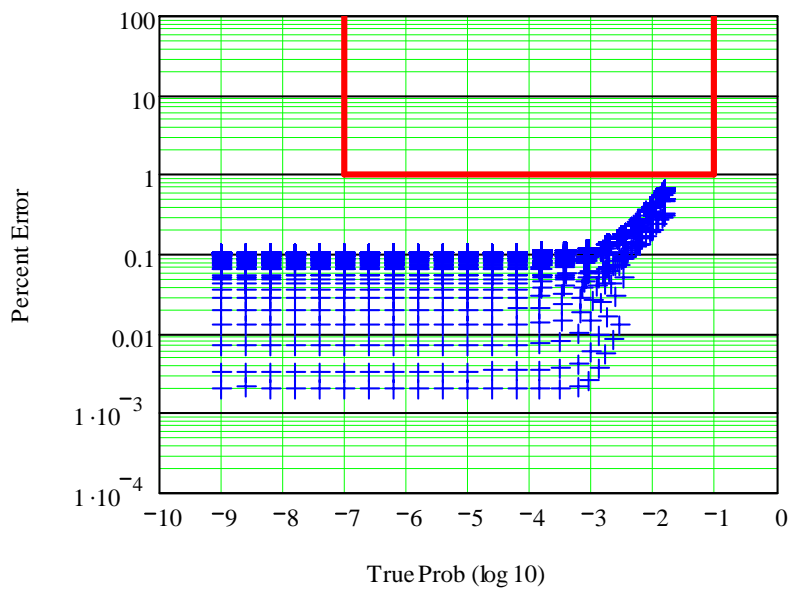


CHAN Method (m=10 unfiltered) AR = 500

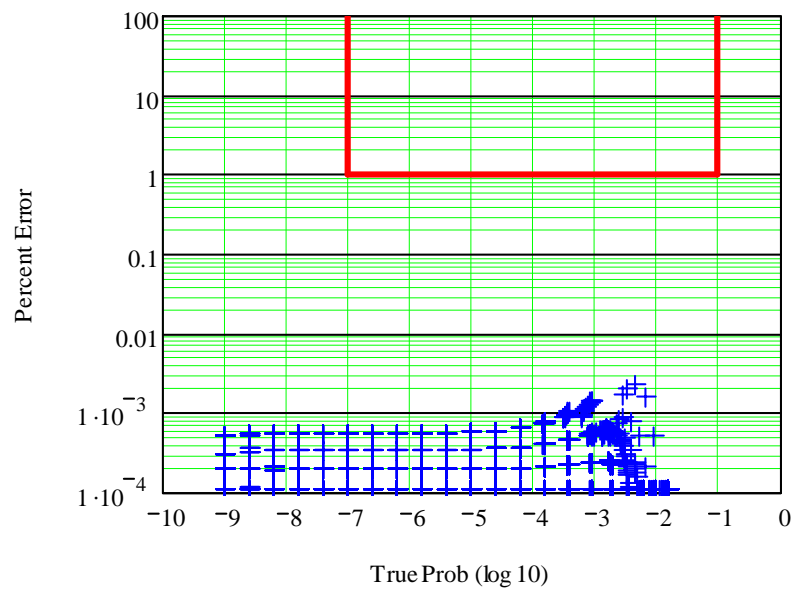


OBJ > DIST AR=500

PATERA 2001 Method N=2000 AR = 500



ALFANO Method AR = 500



Appendix B

Foster method filtered results

Chan method filtered results

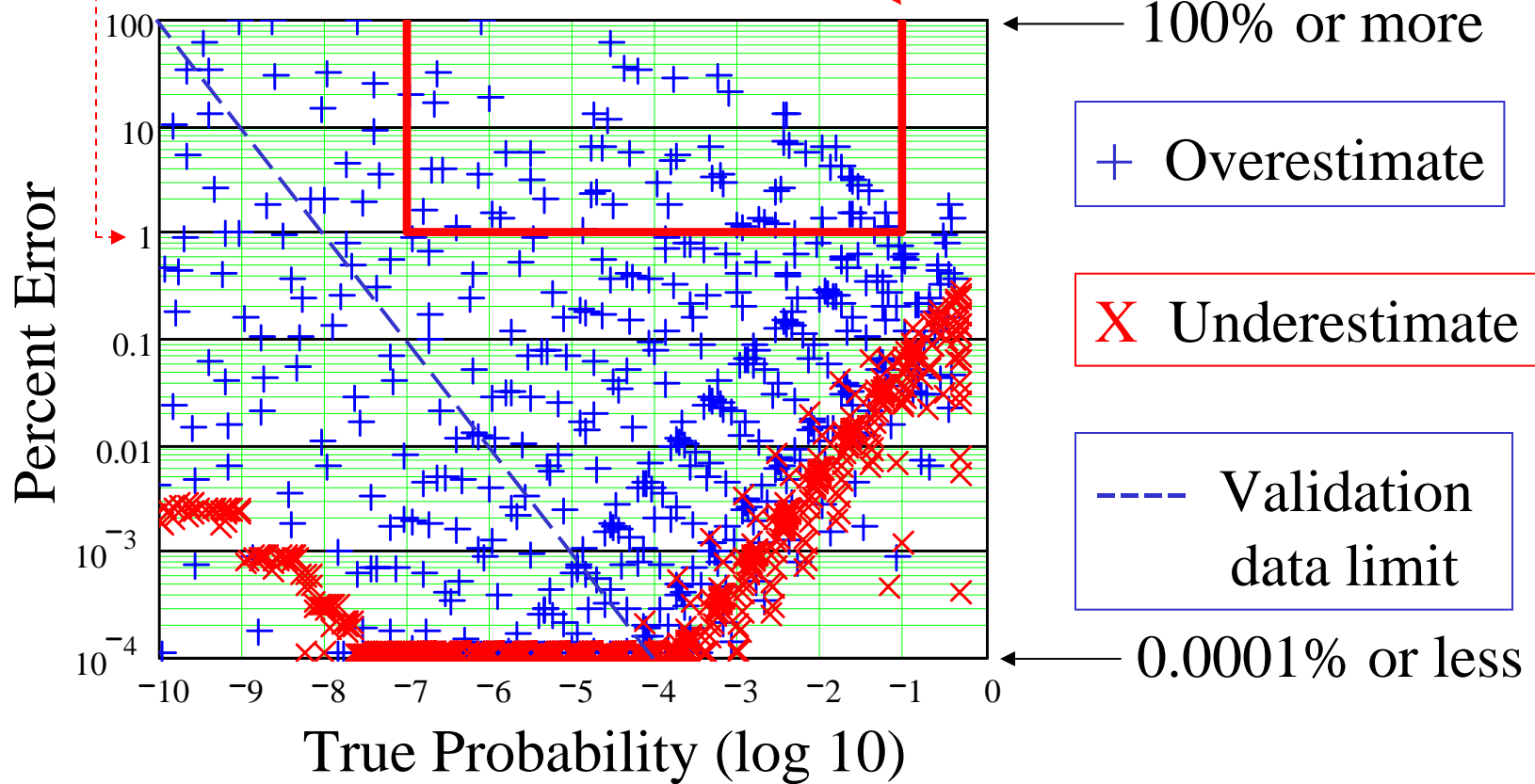
Patera 2005 method results

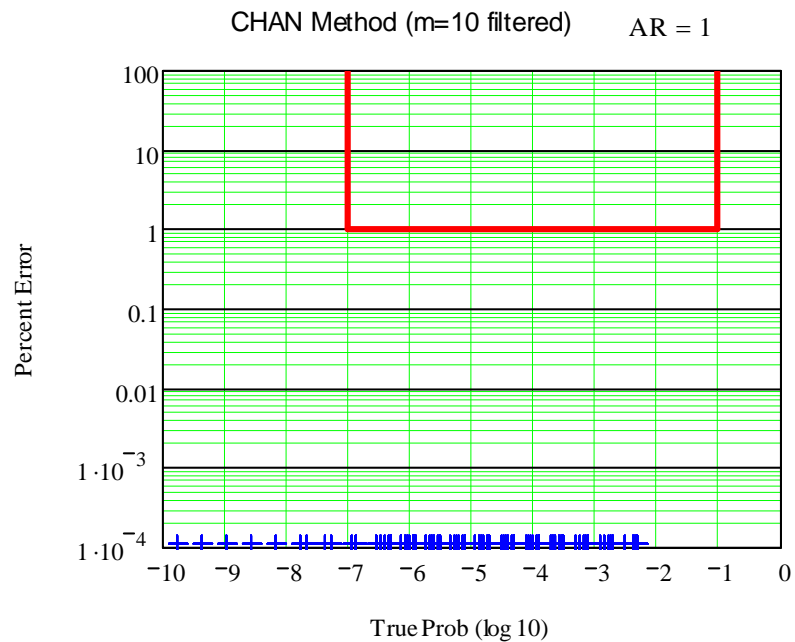
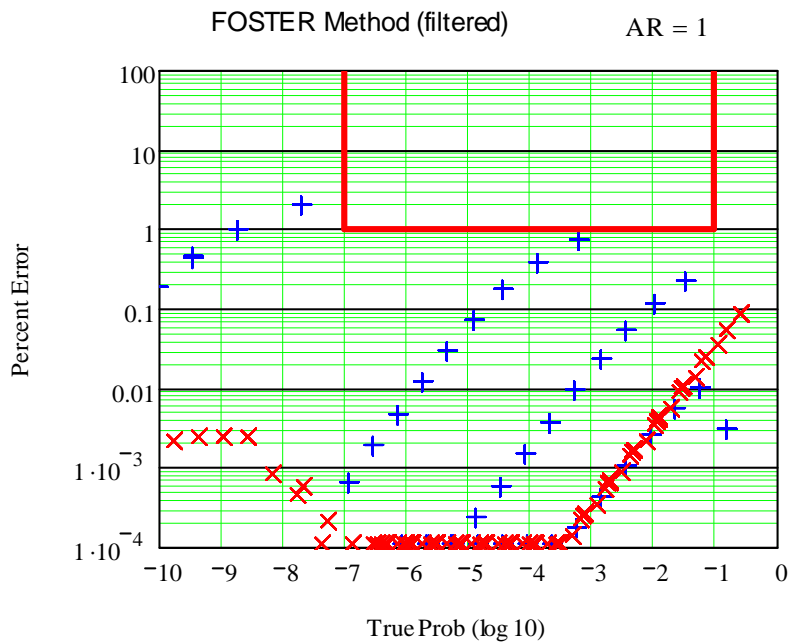
Legend

Slide layout
FOSTER CHAN
PATERA

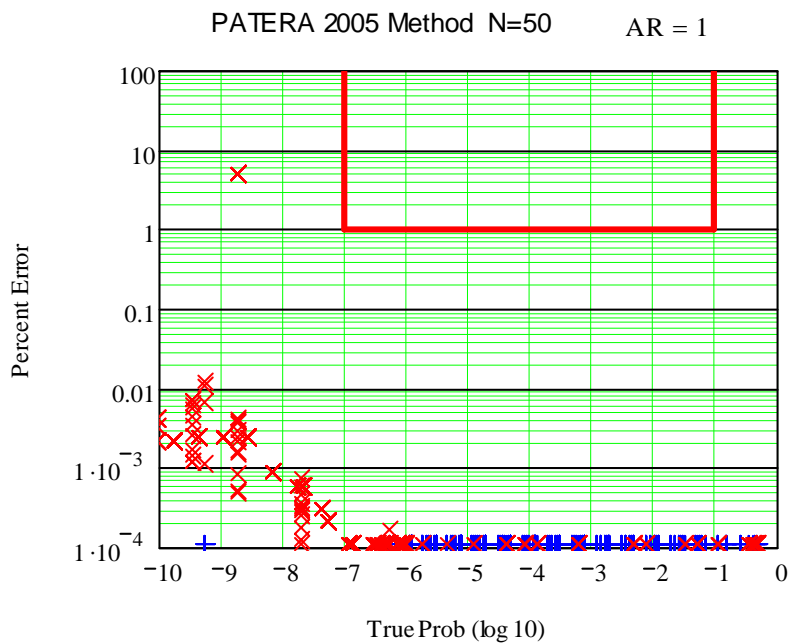
Operational decision making region

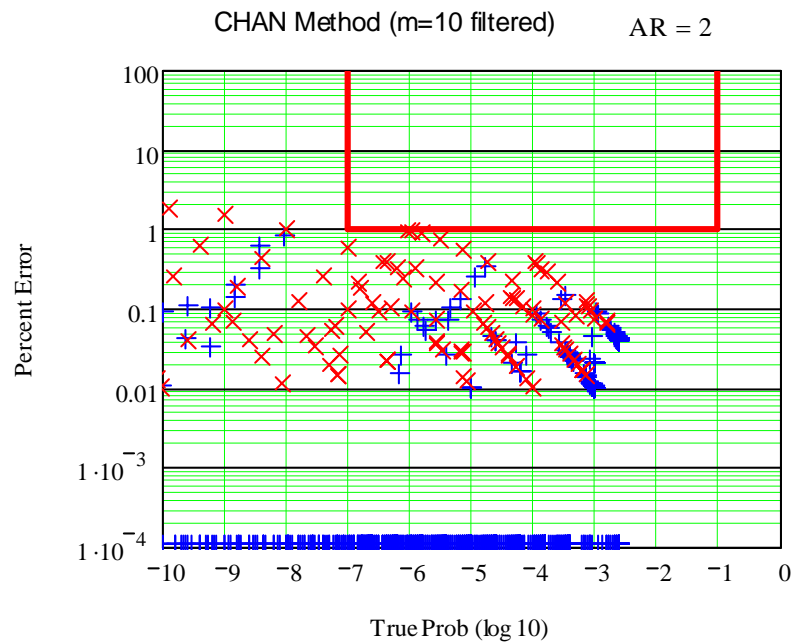
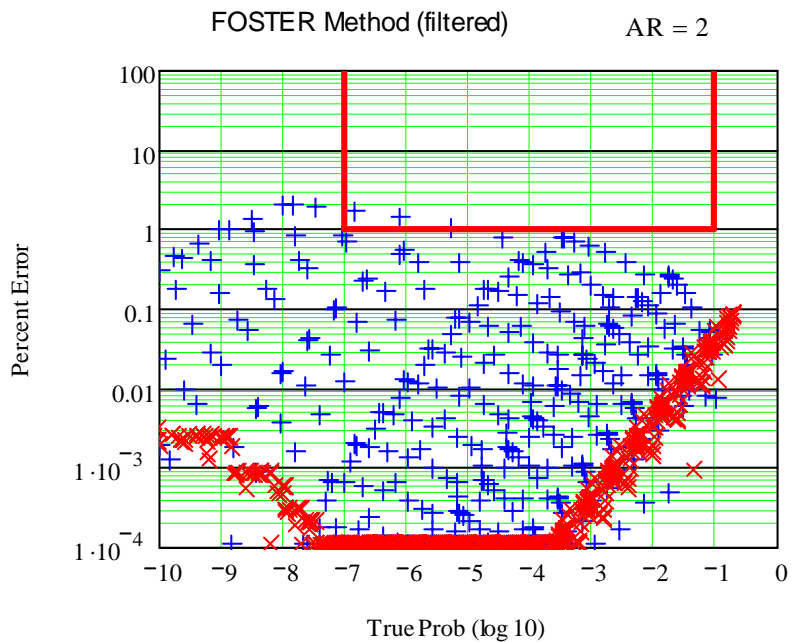
1% error for $10^{-7} < P < 10^{-1}$



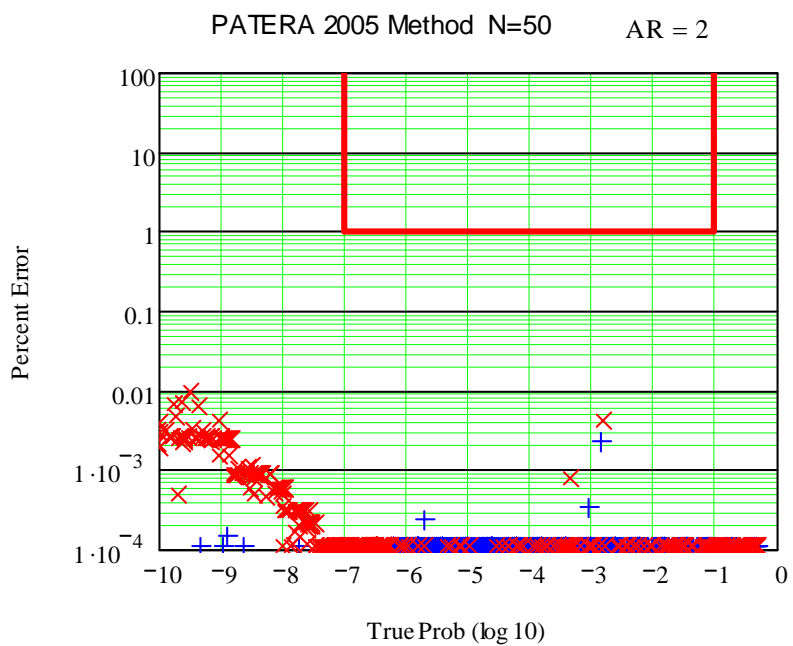


OBJ \leq DIST AR=1

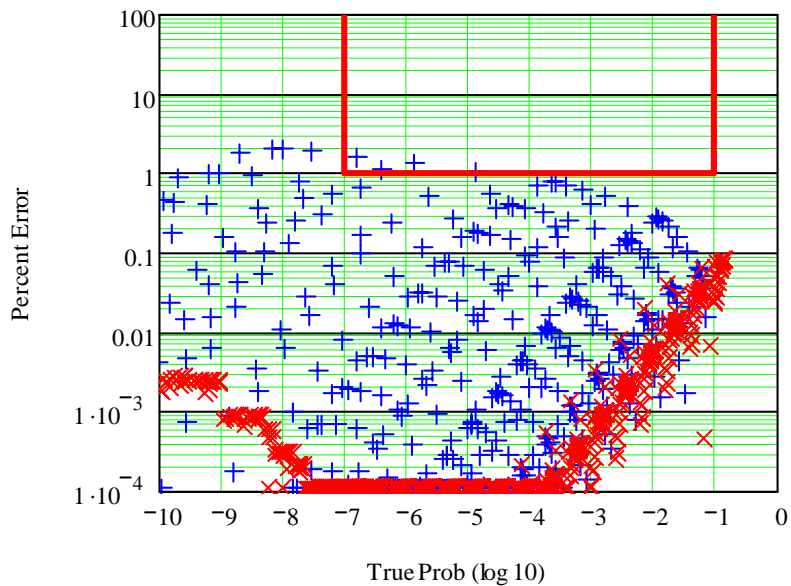




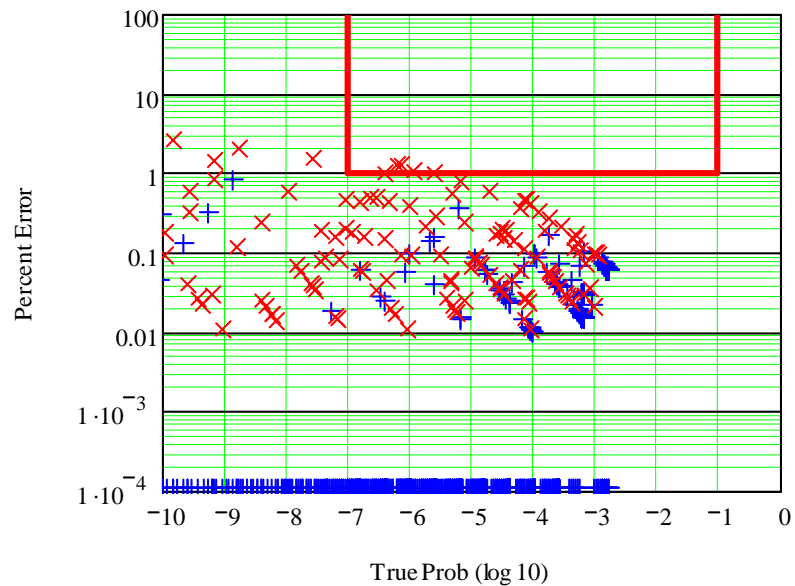
OBJ \leq DIST AR=2



FOSTER Method (filtered) AR = 3

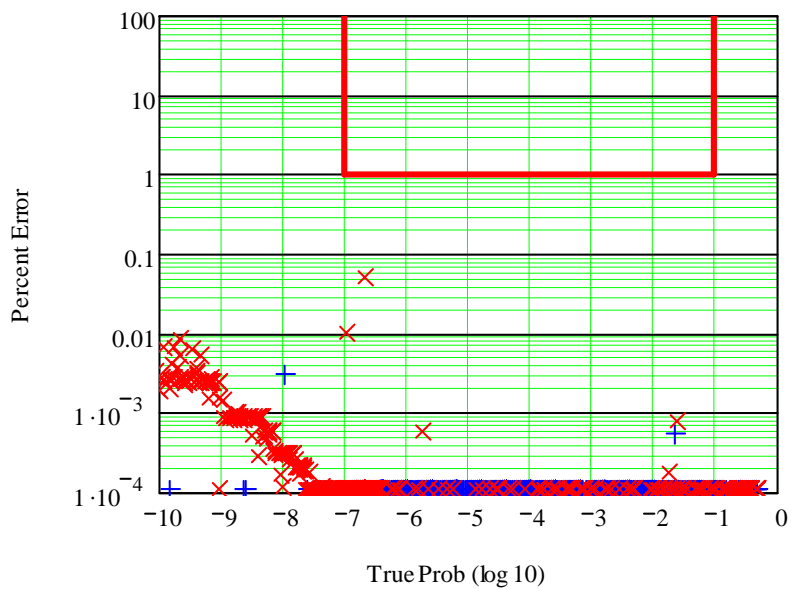


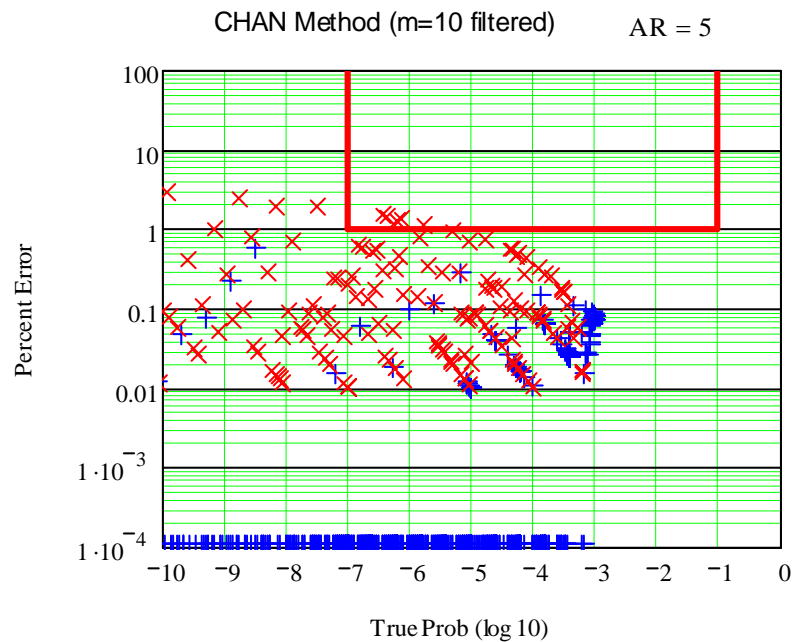
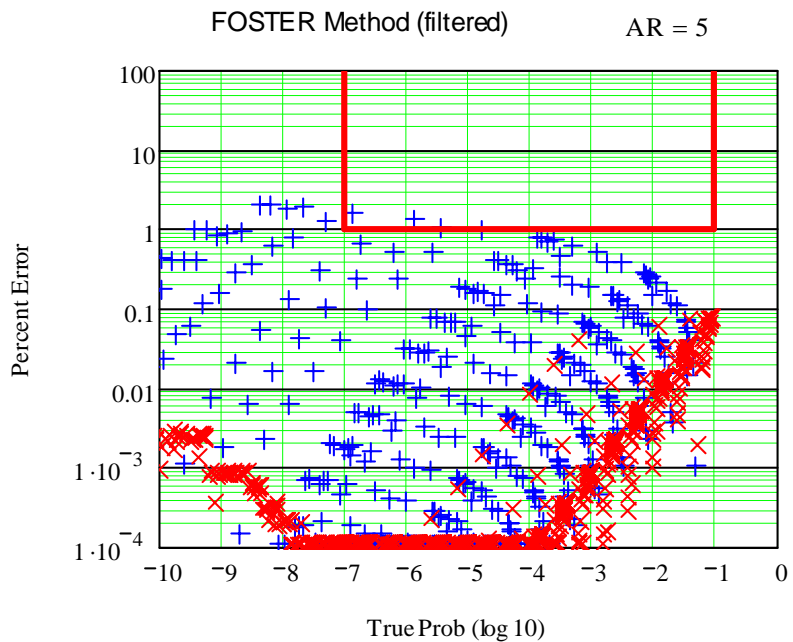
CHAN Method (m=10 filtered) AR = 3



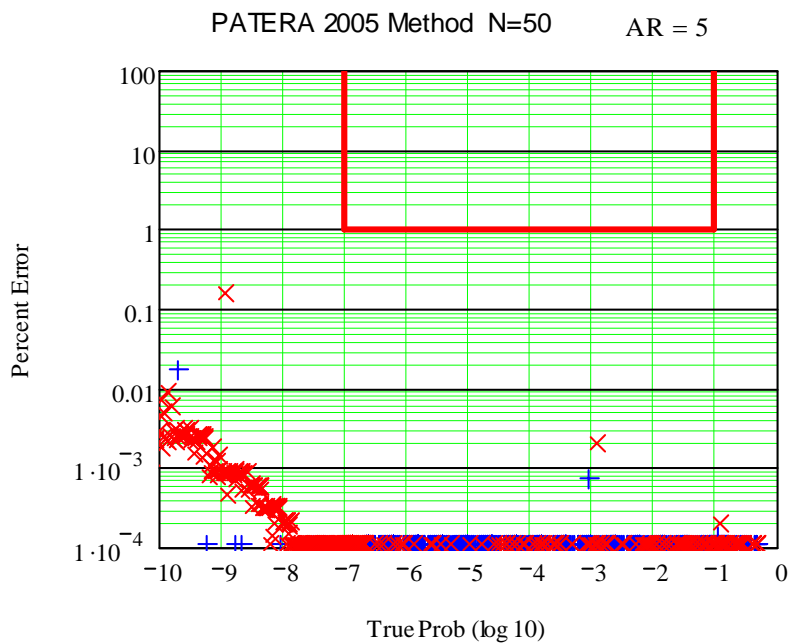
OBJ <= DIST AR=3

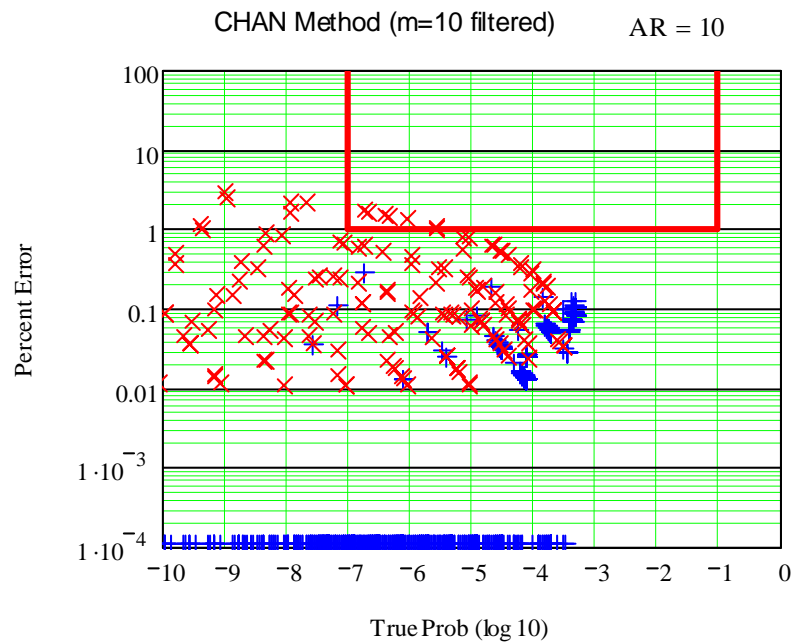
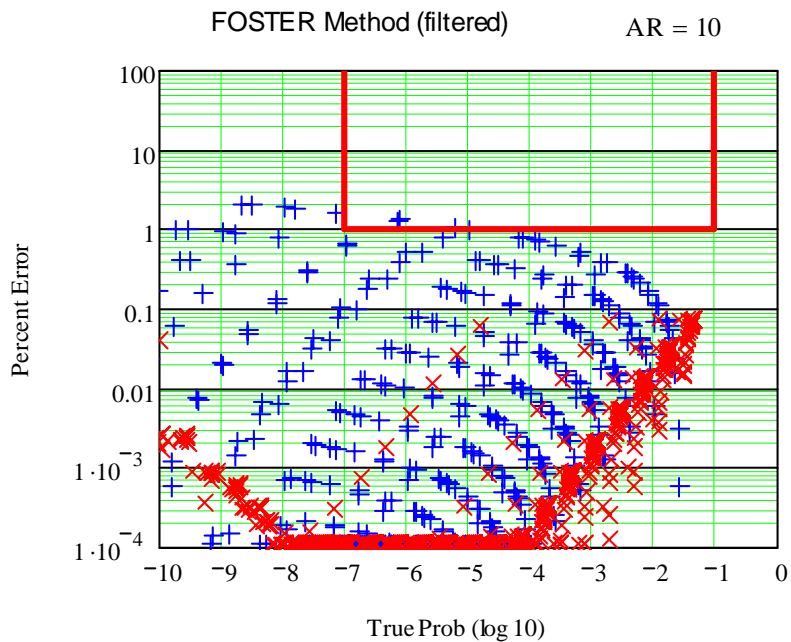
PATERA 2005 Method N=50 AR = 3



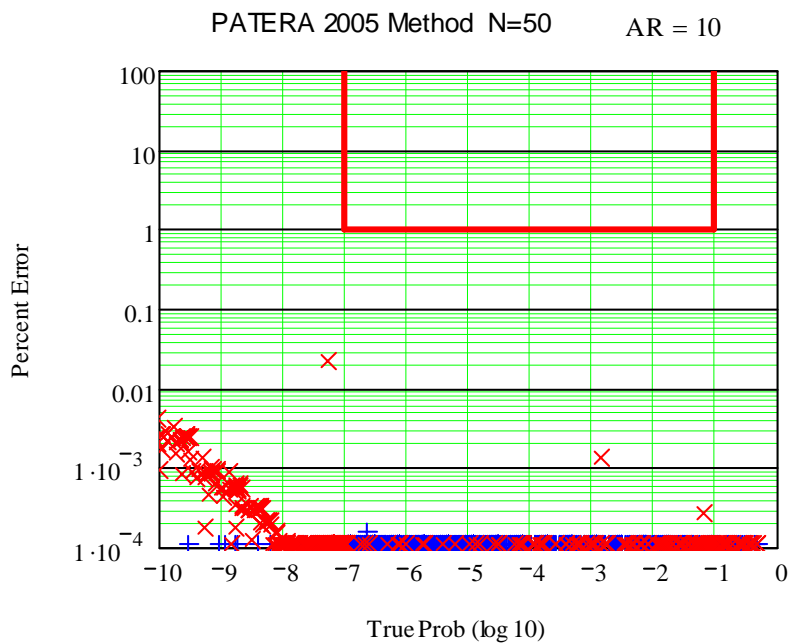


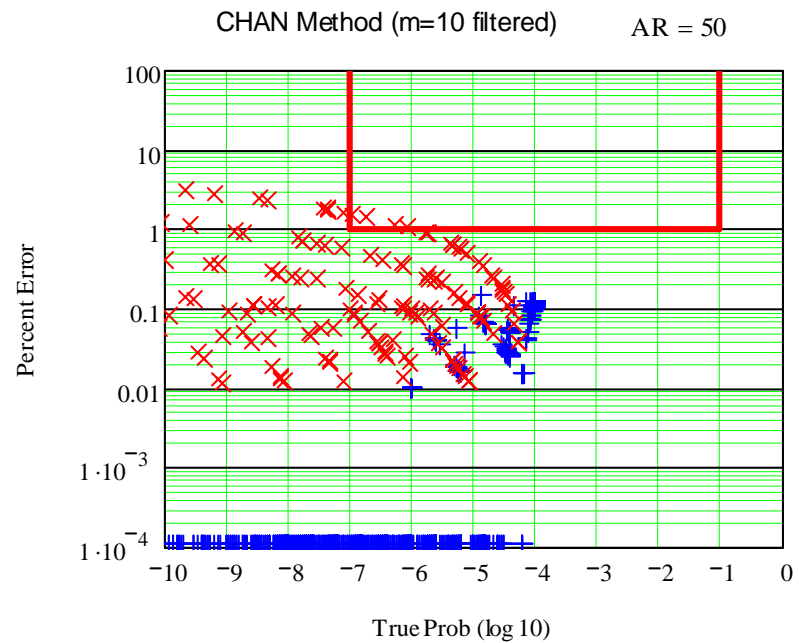
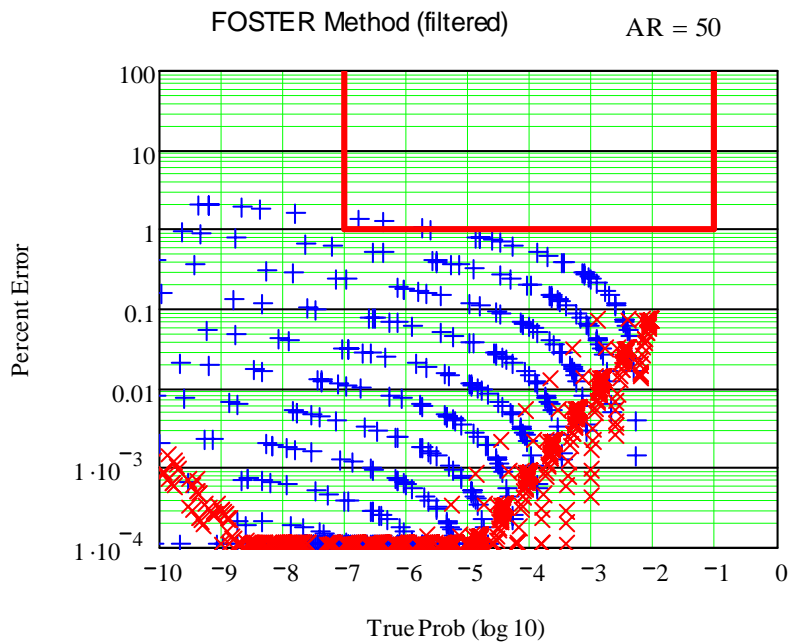
OBJ \leq DIST AR=5



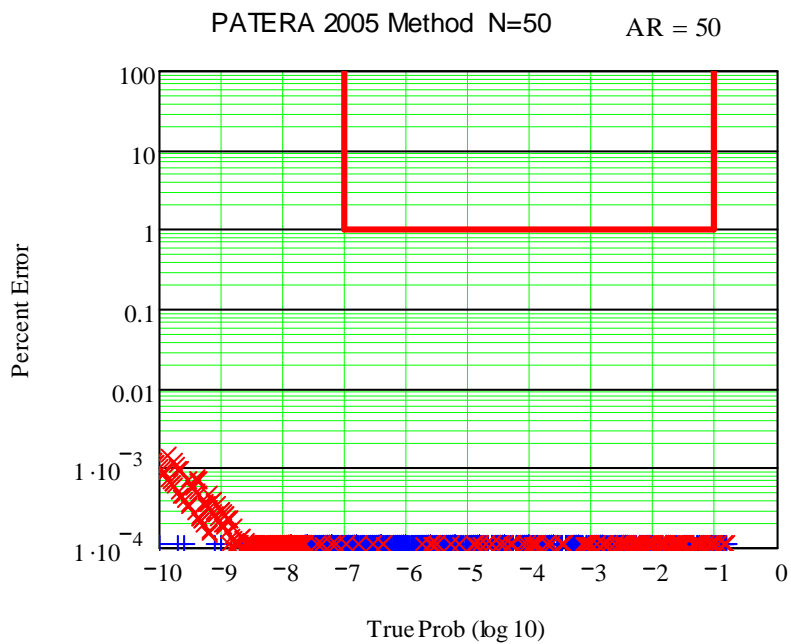


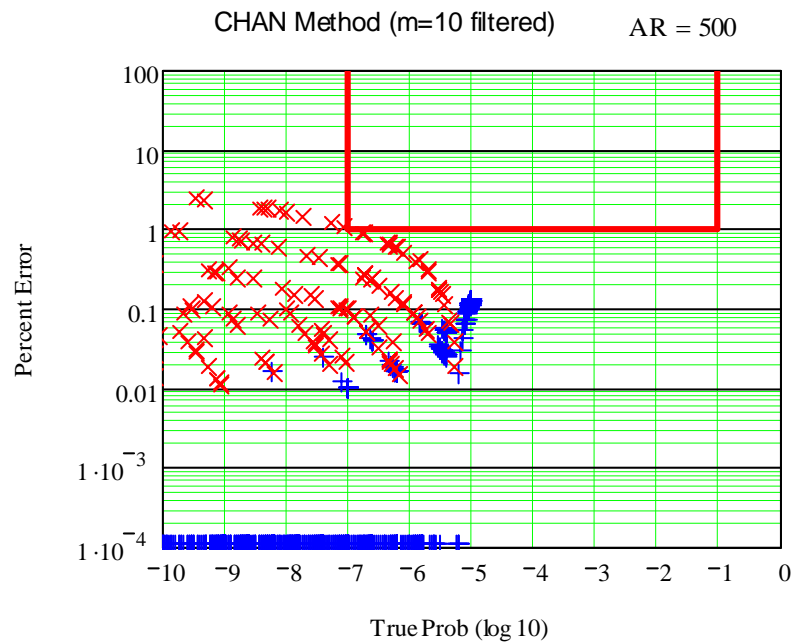
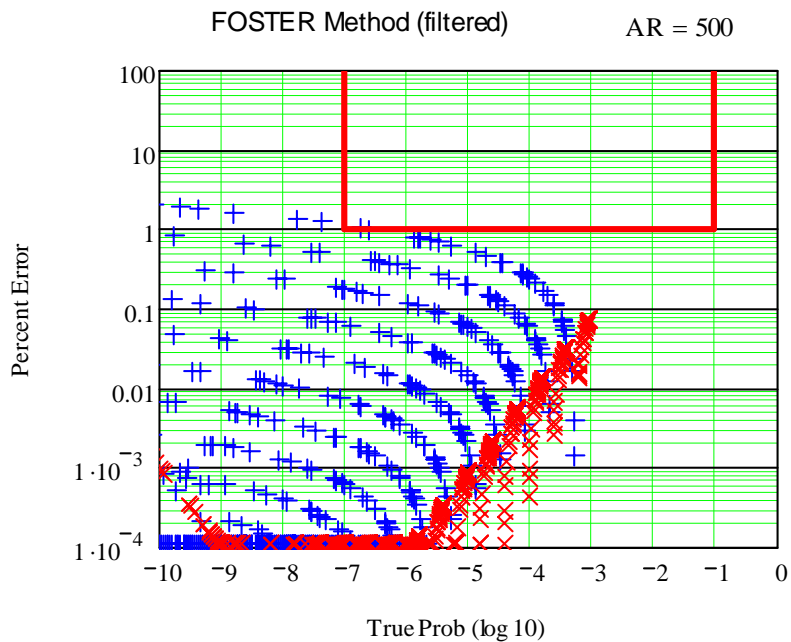
OBJ \leq DIST AR=10



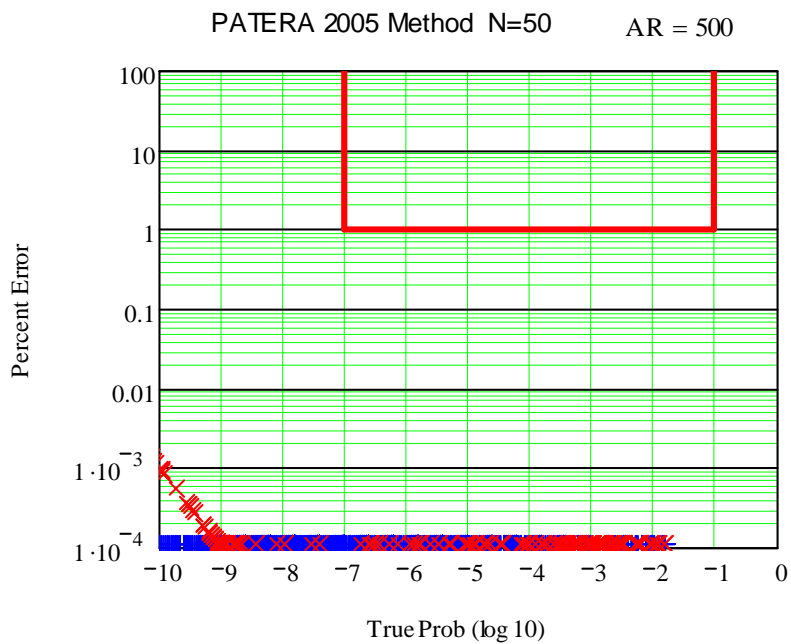


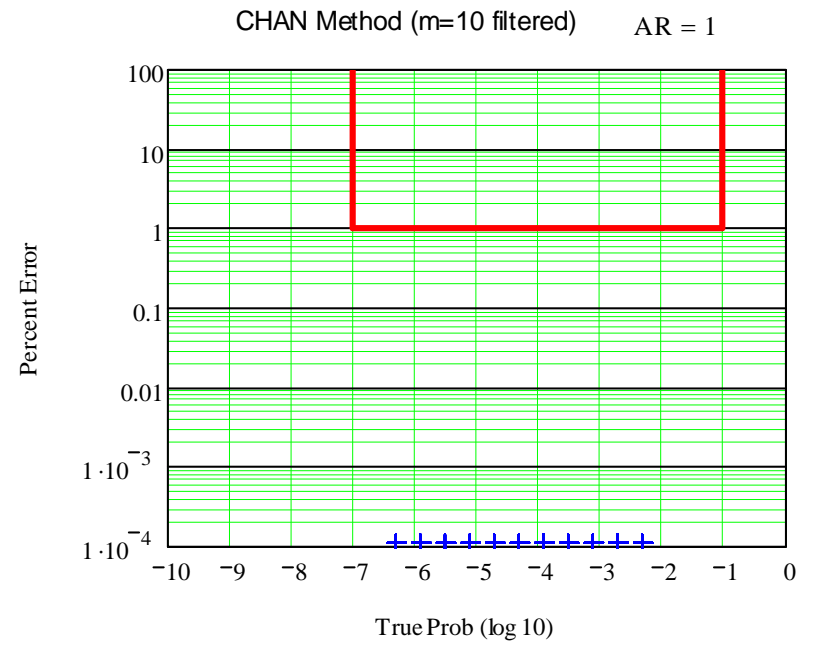
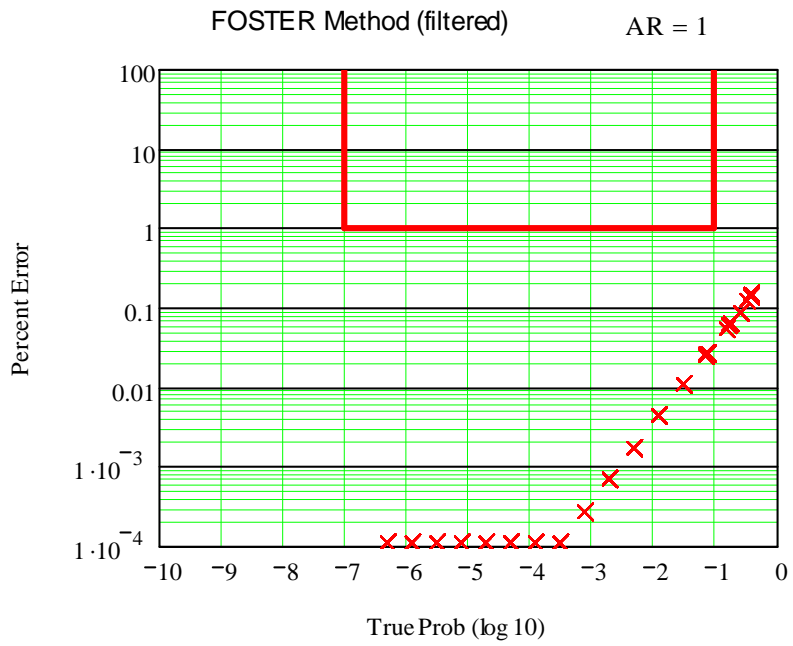
OBJ \leq DIST AR=50



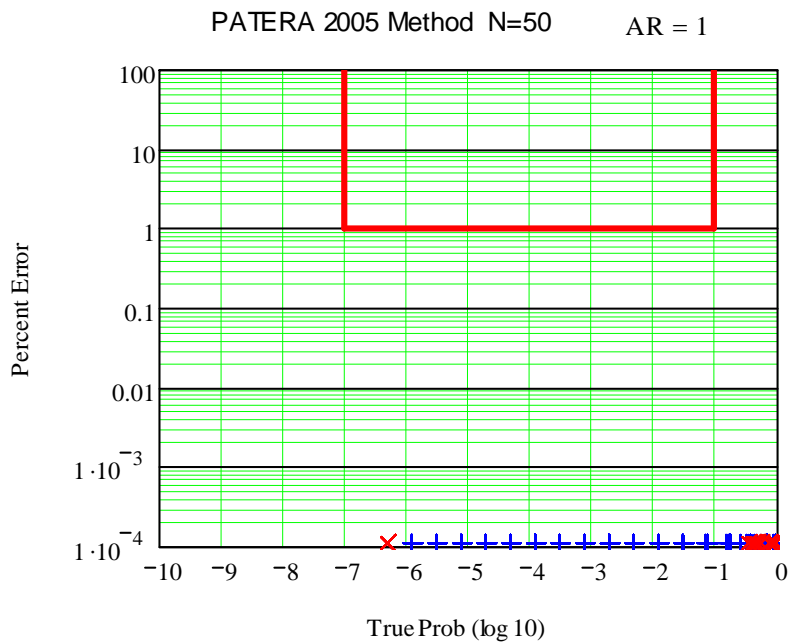


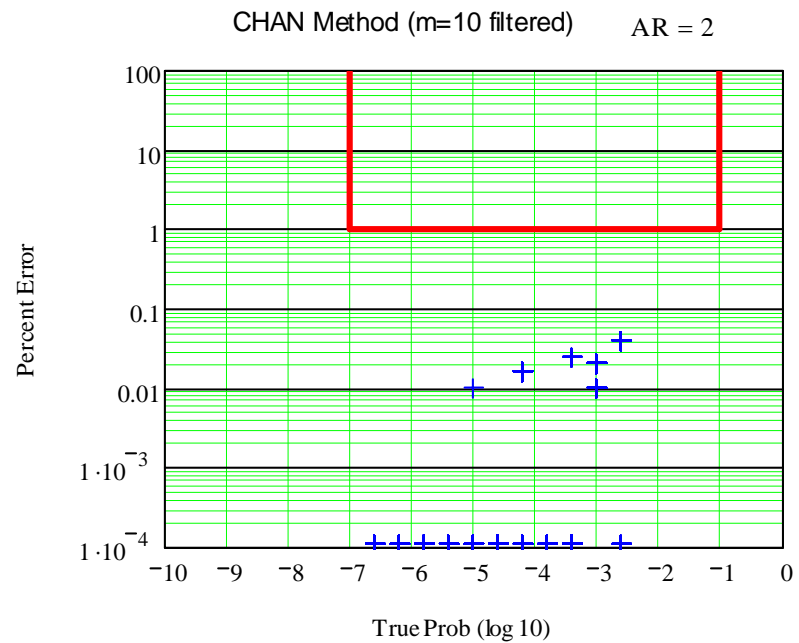
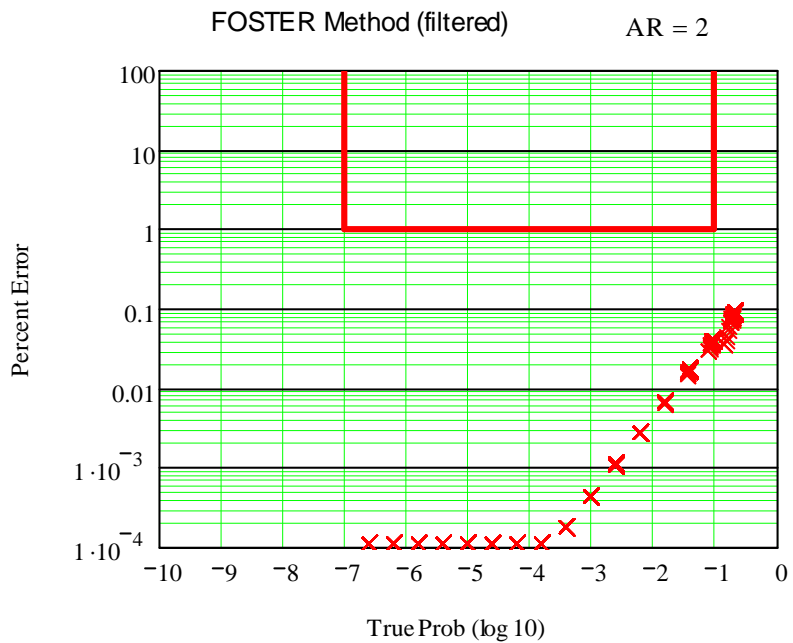
OBJ \leq DIST AR=500



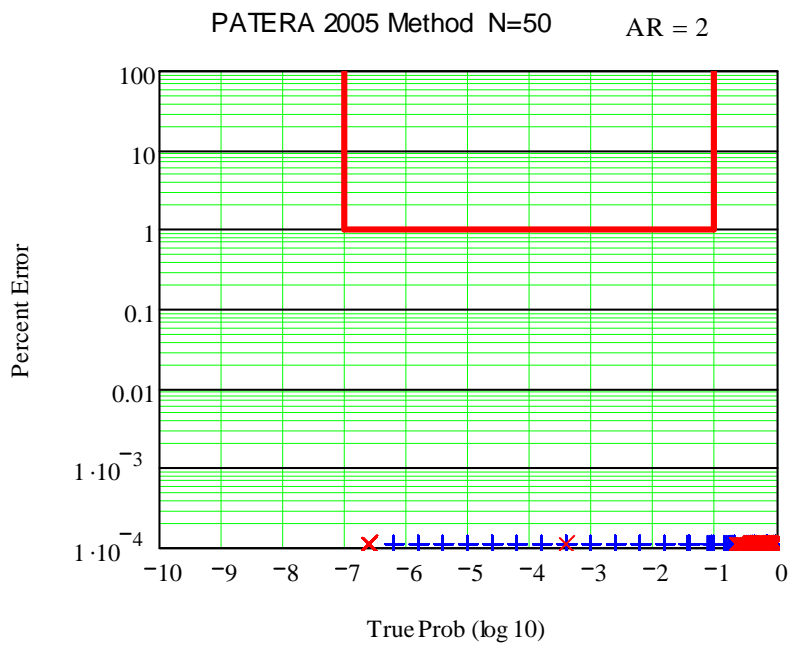


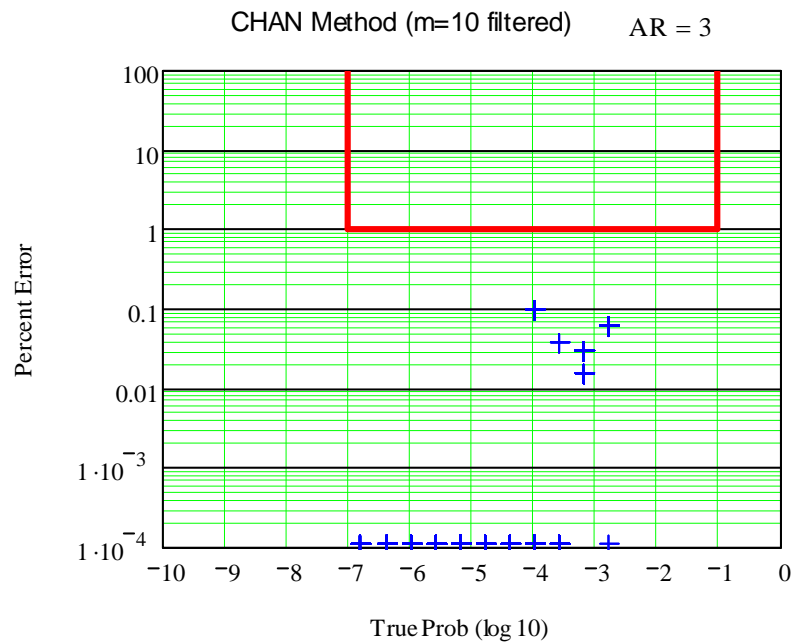
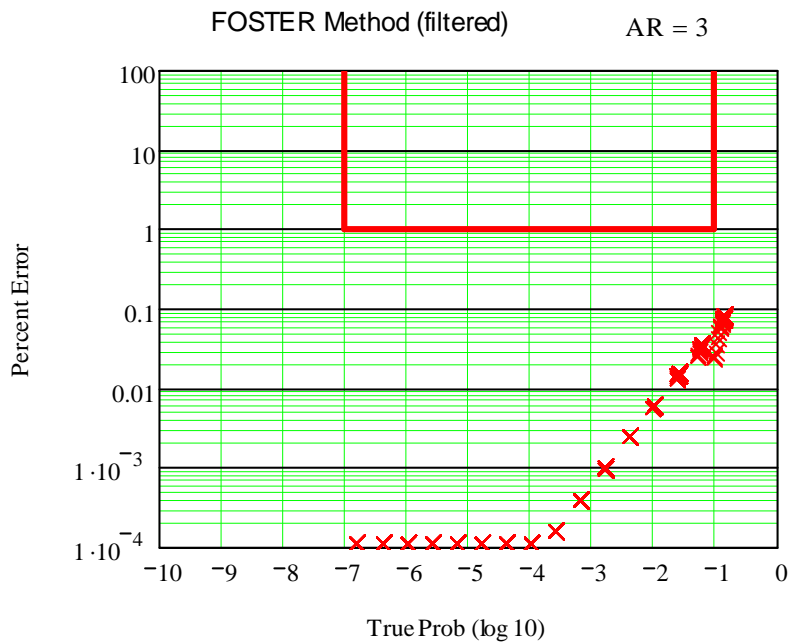
OBJ > DIST AR=1



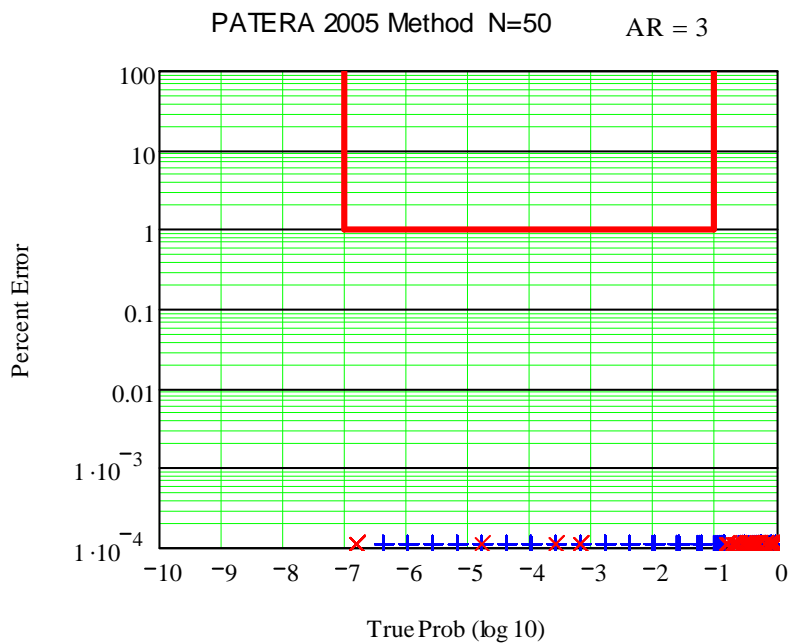


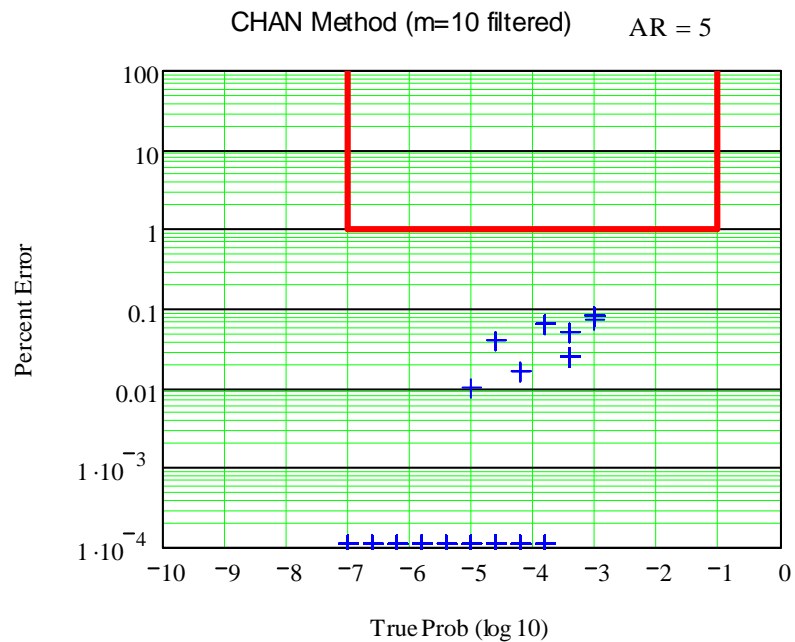
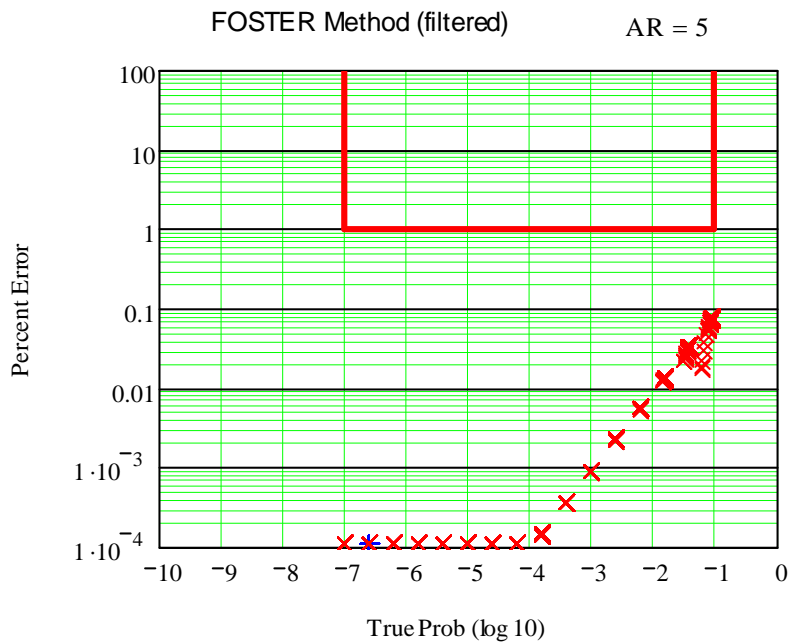
OBJ > DIST AR=2



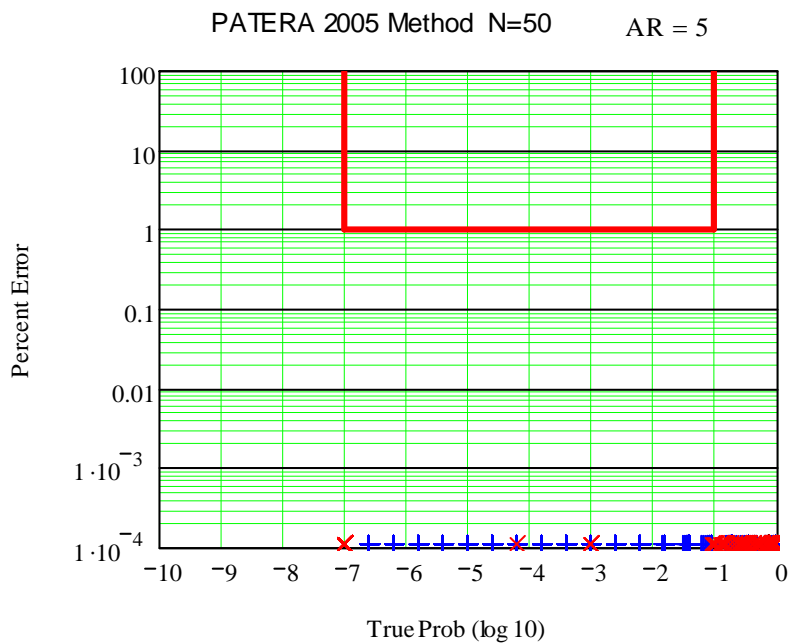


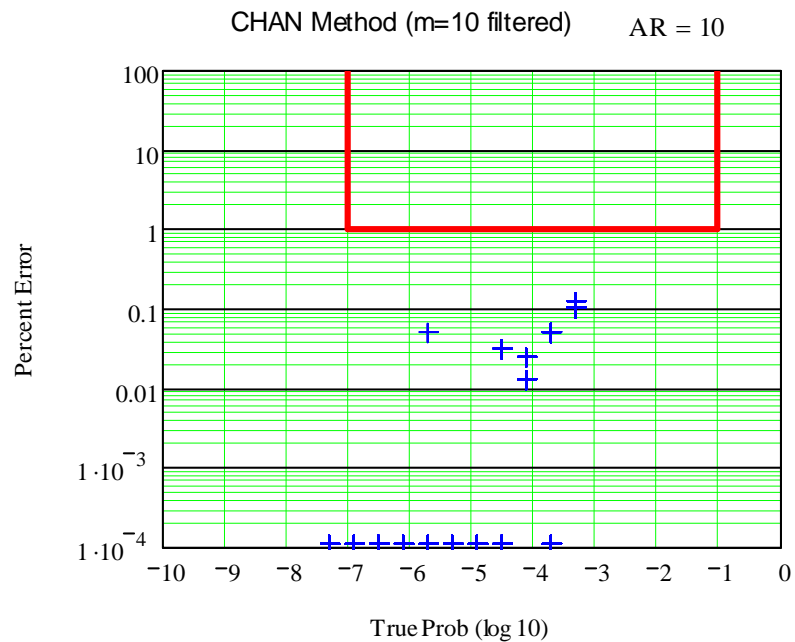
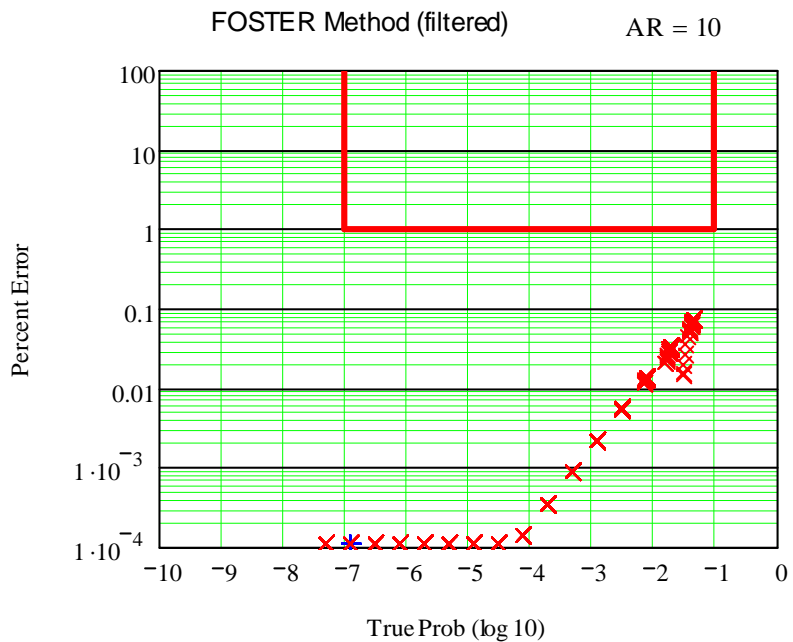
OBJ > DIST AR=3



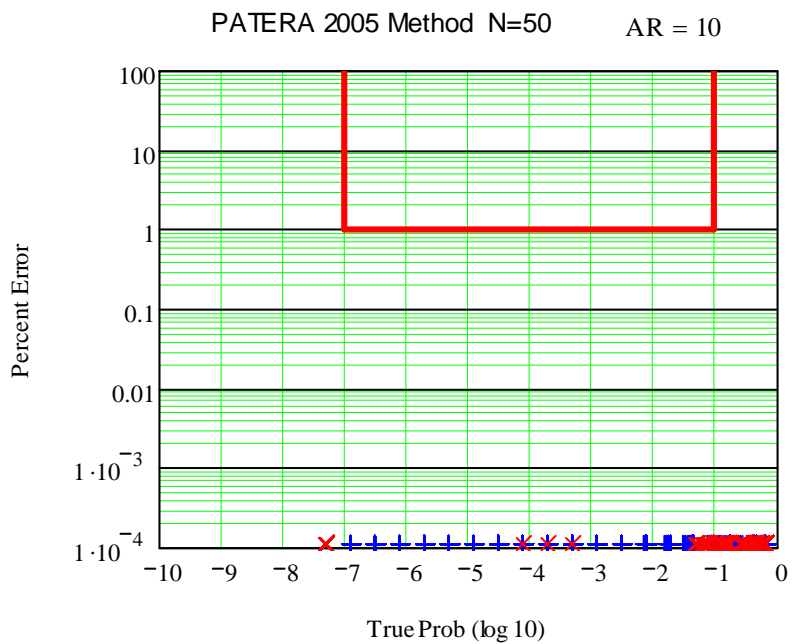


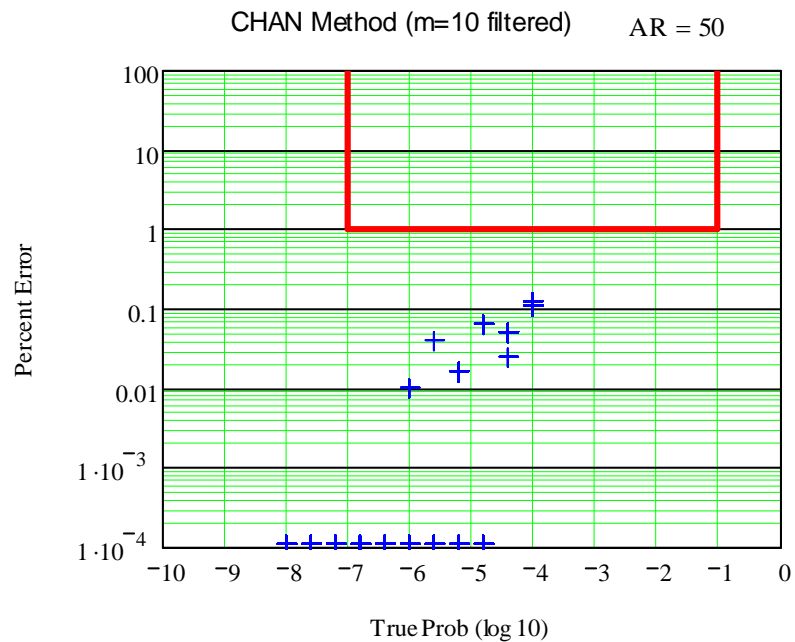
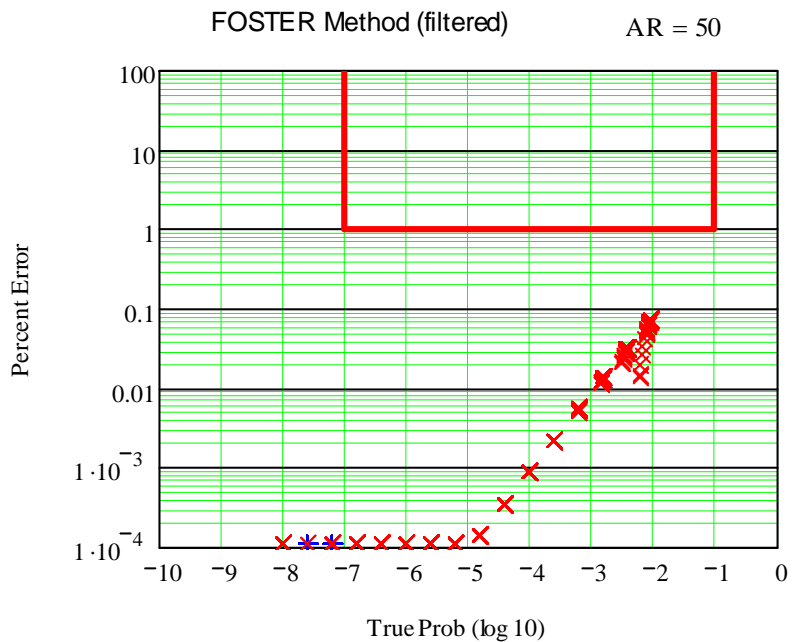
OBJ > DIST AR=5



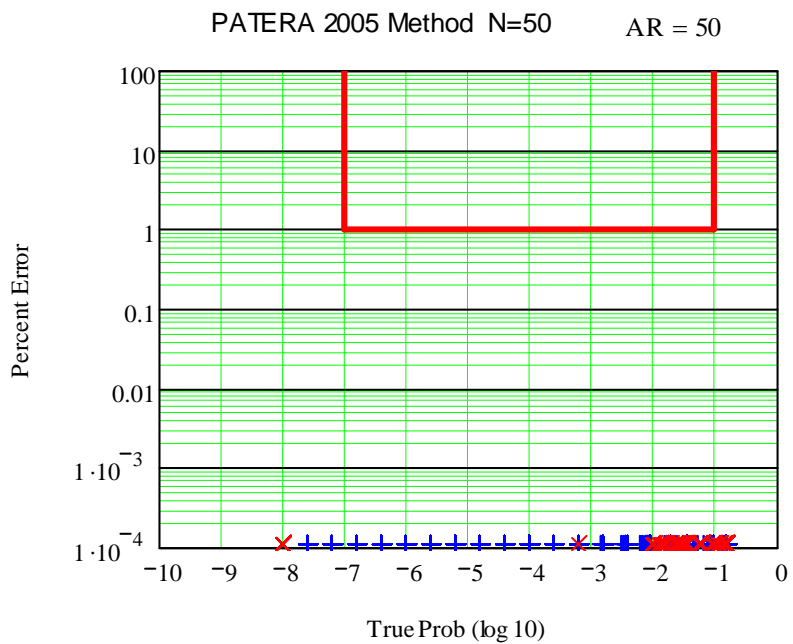


OBJ > DIST AR=10

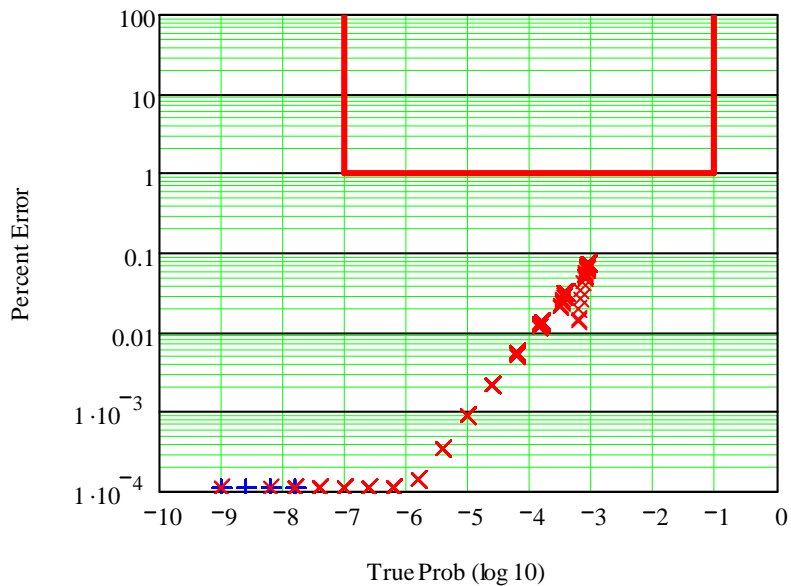




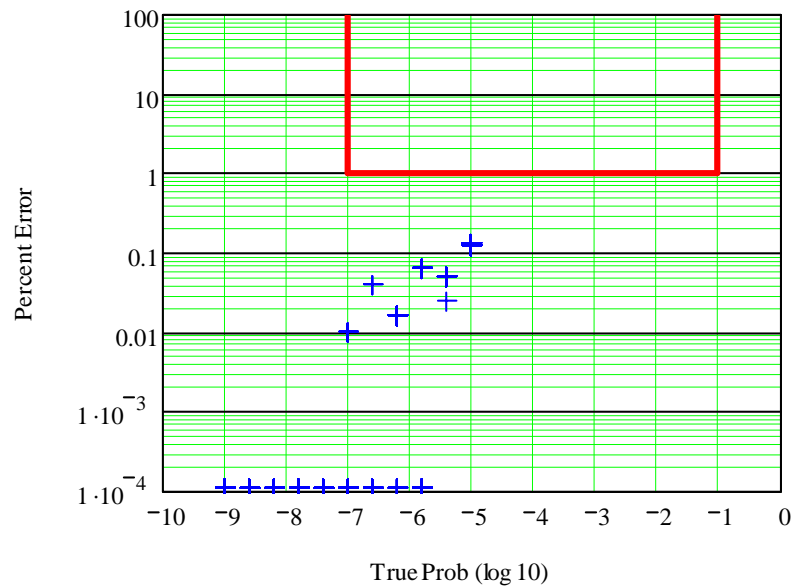
OBJ > DIST AR=50



FOSTER Method (filtered) AR = 500



CHAN Method (m=10 filtered) AR = 500



OBJ > DIST AR=500

PATERA 2005 Method N=50 AR = 500

